TESTING THE RELIABILITY AND SELECTIVITY OF DIFFERENT BONE-CELL-SPECIFIC CRE-EXPRESSING MOUSE MODELS FOR STUDYING BONE CELL METABOLISM

Anuradha Valiya Kambrath

Submitted to the faculty of the University Graduate School
in partial fulfilment of the requirements
for the degree
Master of Science
in the Department of Biochemistry and Molecular Biology,
Indiana University

May 2015

Accepted by the Graduate Faculty, Indiana University, in partial fulfillment of the requirements for the degree of Master of Science.

Master's Thesis Committee

_____

Robling G Alexander, Ph.D., Chair

_____

Goebl G Mark, Ph.D.

_____

Harrington A Maureen, Ph.D.

Dedication

I would like to dedicate this work to my family and friends with whose love and support made this project a possibility.

Acknowledgments

I would like to thank my mentor, Dr. Alexander Robling for his guidance and also for providing materials and methodology support of this work. I would like to express my sincere thanks to all the lab members of Dr. Robling, for their timely help. I would like to thank Dr. Jayaram Hiremagalur for his support and mentorship during this project. I would like to thank Dr. Mark Goebl for his continuous support and guidance throughout the duration of this project. I would also like to thank Dr. Maureen Harrington, my thesis committee member for her support. Finally I would like to thank Dr. Rajendra Kedlaya for his technical assistance and support during this project.

Anuradha Valiya Kambrath

TESTING THE RELIABILITY AND SELECTIVITY OF DIFFERENT BONE-CELL -SPECIFIC CRE-EXPRESSING MOUSE MODELS FOR STUDYING BONE CELL METABOLISM

The Cre/loxP system is a tool for targeted recombination of DNA. For applying Cre recombinase-mediated genome modifications, there is a requirement for reliable, high-fidelity, and specific transgenic expression of the Cre recombinase. This study focuses on the reliability of different bone cell specific Cre models in the Cre/loxP system. In this study, *DMP1-Cre* transgenic mouse which has a transgene driven by DMP1 promotor that allows Cre-expression only in late stage osteoblasts and osteocytes was used. *Ctsk-Cre* mouse with a driven by Ctsk promoter was used so that only osteoclasts would undergo Cre-mediated recombination. *E2A-Cre* mouse where the Cre recombinase is driven by a global promoter E2A was also included in this study as a control line to test the Cre reporter line *Ai9*. *Dmp1-Cre, Ctsk-Cre* and *E2A-Cre* mice were crossed to the fluorescent Cre-reporter line—*Ai9*, which harbors a floxed stop codon, followed by the fluorophoremTomato, inserted into the Rosa26 locus. This construct is expected to give red fluorescence when it recombines with Cre-expressing mouse cells and no fluorescence in non-recombinant mouse cells. Double positive (*Ai9+/Cre+)* offspring selected by PCR were perfused, and 5µm thick section of bone and soft tissues were examined for red fluorescent expression. Cre positive cells were quantitated using ‘ImageJ’ software program. The *DMP1-*

Cre mouse results showed significant expression in the targeted osteocytes and osteoblasts. In addition, skeletal muscle tissue also showed significant Cre-expression. *Ctsk-Cre* mice showed significant expression in targeted osteoclasts. But brain tissue was positive in Cre-expression. *Bone-Cre* mouse models are expected to express Cre recombinase only in their respective bone cells and they have been used for gene deletion studies in bone cells. However, this study has revealed that the bone cell specific Cre mouse models *DMP1-Cre* and *Ctsk-Cre* have unexpected expression in muscle and brain respectively. In order to use these models for targeted gene deletion in bone cells, further testing and studies have to be conducted.

Robling G Alexander, Ph.D., Chair

Table of Contents

List of Tables

List of Figures

Abbreviations

Cre:	Cre-recombinase
DMP1:	Dentin Matrix Protein1
Ctsk:	Cathepsin K
PCR:	Polymerase Chain Reaction
Ert2:	Estrogen receptor 2
Trap:	Tartarate resistant acid phosphatase
DAPI:	4′, 6-Diamidino-2-phenylindole dihydrochloride
PBF:	Phosphate buffered formalin
OCT:	Optimal cutting temperature compound
SCMM:	Super Cryo mounting medium.
H&E stain:	Haematoxylin and Eosin stain
HotSHOT:	Hot Sodium Hydroxide and Tris
EDTA:	Ethylene diamine tetra acetic acid
NaOH:	Sodium hydroxide
HCl:	Hydrochloric acid
TAE:	Tris-acetate-EDTA
TBE:	Tris-borate-EDTA
ITCN:	Image based tool for counting nuclei

1. Background

Aim:

To determine the tissue specificity and reliability of different Cre-expressing mouse models, to better understand the body-wide (off-target) effects of floxed gene recombination in ‘bone-specific’ models of Cre expression.

Genetic mouse models are valuable tools for scientific research and discovery. Deletion of a specific gene could reveal role of a particular protein or even the entire signaling pathway involved in disease and health. Thus genetic deletion has become a relatively straight forward and routine practice in biomedical sciences. However, there are limitations for conventional gene knockout strategies which made them difficult to apply in research contexts. Conventional (germ line) knockout can produce a lethal phenotype, precluding the study of that gene or pathway in a postnatal system. Also certain genes can have diverse effects across tissues, so it is difficult to study the effect of genetic deletion on the phenotype in the context of an isolated tissue or organ system. The Cre/loxP system is a tool that has been developed to solve some of these problems and it has expanded our ability to conduct studies.

1.1. Cre/loxP system:

The Cre/loxP system is a tool for site specific recombination of DNA. This recombination system is originated from lytic cycle of P1 bacteriophage in *E coli*.

Cre/loxP recombination is a natural process that occurs in the life cycle of P1 bacteriophage which plays two important roles. The first role involves circularization of P1 DNA when it enters the host.10-20% of P1 DNA is terminally redundant and some of the entering P1 DNA molecules contain two loxP sites and can be efficiently circularized by Cre. The second role involves the breakdown of dimer P1 DNA molecules that may form as a result of replication or homologous recombination [1]. When a DNA containing the loxP site is incubated with Cre, a specific cleavage occurs within the spacer region, creating a six base-pair staggered cut. The cuts are centered on the axis of dyad symmetry of the loxP site, resulting in a 5′ protruding terminus: $^{5'}$ A↓T-G-T-A-T-G C/ $^{3'}$ T A-C-A-T-A-C↑G At the point of cleavage, Cre becomes covalently attached to a 3′ PO_4, and produces a free 5′ OH [2]. The Cre/loxP system is functional in both bacteria and eukaryotic cells and has been used for the excision and the integration of fragments in cellular and viral genomes. It has been exploited in cell-free systems for construction of recombinant vectors [3]. This system is also useful for genetic knockout or knock-in in animal models when a conventional knockout produces (a) lethal phenotype, or (b) when conventional knockout is viable but tissue-specific effects are desired [5]. *In vivo*, two mouse lines are required for conditional gene deletion using the Cre/loxP system. The first mouse model required is one that expresses the coding sequence for *Cre* transgene, under the control of a promoter that has the desired tissue or cell-type selectivity. Cre is a tyrosine recombinase isolated from the P1 bacteriophage, which recognizes and cleaves the 34 base pair loxP sequence. The second mouse

model harbors a modification of the gene of interest, such that a crucial portion of the coding sequence is flanked by loxP sequences, which resides in the non-coding introns. This gene, once the loxP sequences are introduced, is said to be 'floxed'. The introduction of loxP sequences into the intronic regions does not have an effect on target gene transcription [5, 6, 7]. Recombination (excision and consequently inactivation of the target gene) occurs only in those cells expressing Cre recombinase. Hence, the target gene remains active in all cells and tissues which do not express Cre [4, 5].

1.2. Cre recombinase:

The Cre recombinase is an integrase family of enzyme derived from P1 bacteriophage [5]. This enzyme is a tyrosine recombinase and catalyzes the site specific recombination of DNA between two loxP sites. The enzyme does not require any co-factors and Cre-mediated recombination quickly reaches equilibrium between substrate and products. The loxP recognition element is a 34 bp sequence which has 13 bp inverted repeats flanking an 8 bp spacer region which is for directionality (Figure 1) [1, 3, 4]. Recombination products depend on the location and relative orientation of the loxP sites. Two DNA fragments containing single loxP sites will be fused, DNA between directly repeated loxP sites will be excised in circular form and DNA between opposing loxP sites will be inverted with respect to external sequences [6]. Cre recombinase is one of the important tools that have made many of the genome alteration technologies possible.

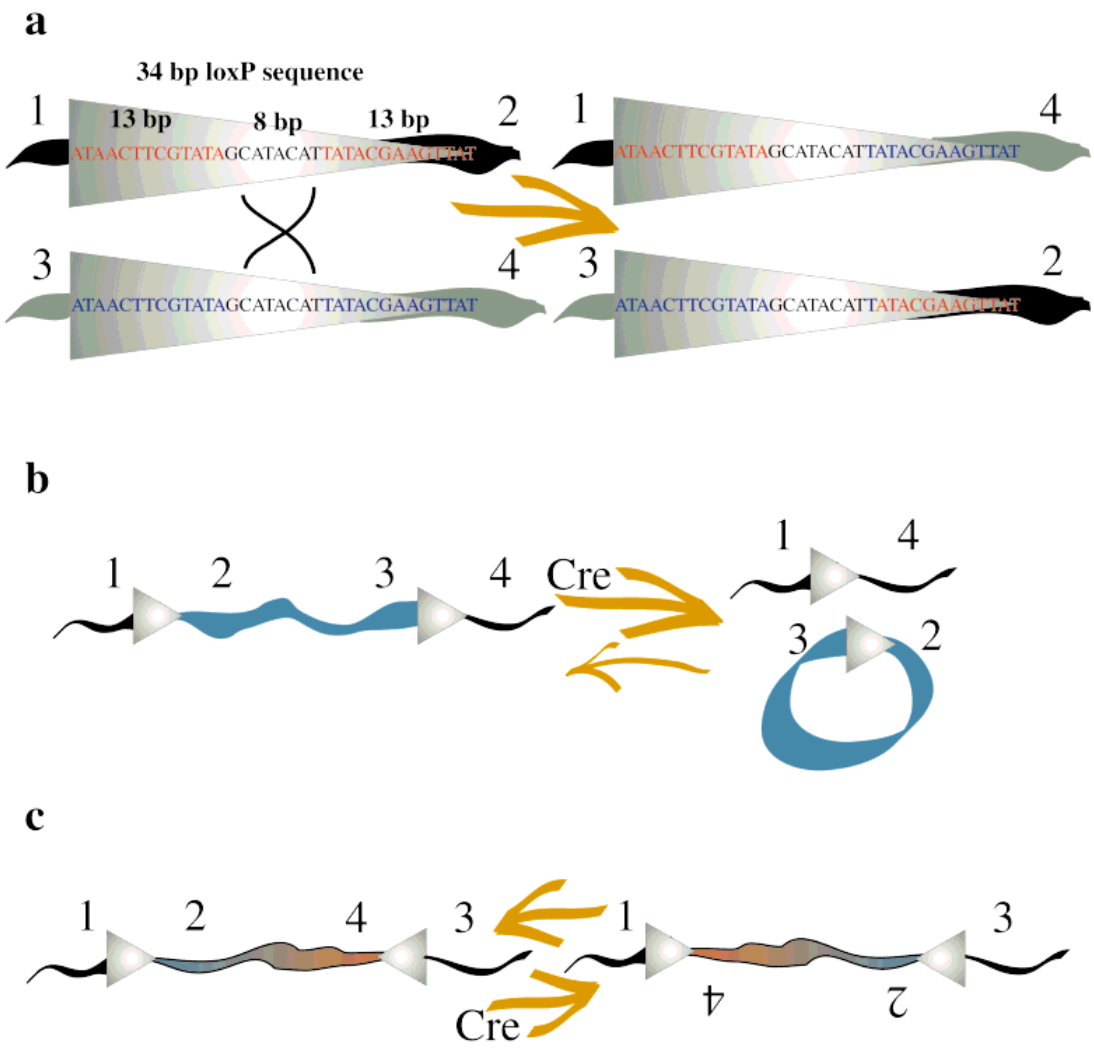

Figure 1: Schematic illustration of Cre/loxP system (from reference 5). (a) Close-up of Cre recombinase-mediated recombination between two 34 bp loxP sites. Nucleotide exchange occurs in between the two loxP sites. (b) When the loxP sequences are in direct repeat, deletion occurs. (c) When the two lopxP sequences are in inverted repeats, inversion occurs.

For applying Cre recombinase-mediated genome modifications, there is a requirement for reliable, high-fidelity and specific transgenic expression of the Cre recombinase. Cre mouse models may not give expected result since many of them are prone to ectopic expression, transgene silencing or genetic background effects [8]. Experimental validation of the Cre line is essential and can be achieved through a combination of molecular and immunohistochemical

approaches. The aim of this study is to test the reliability of different bone cell specific Cre mouse models when they are recombined with floxed genes, so that they could be used as a valuable tool for studying bone cell metabolism.

1.3. Bone cells and bone metabolism:

Bone tissue is maintained by three primary cell types: Osteoblasts, osteocytes and osteoclast. Osteoblasts are bone-forming cells, which are derived from mesenchymal progenitors [9]. The main function of the osteoblast is bone matrix protein secretion and bone mineralization. After completion of bone matrix formation, some mature osteoblasts remain entrapped in bone matrix as osteocytes, some flatten to cover quiescent bone surfaces as bone lining cells and the rest die by apoptosis [10]. Osteocytes or mature bone cells are former osteoblasts that have migrated into, and become trapped and are surrounded by bone matrix. They are regularly distributed throughout the mineralized bone matrix. Osteocytes are the major population of cells in bone. They comprise more than 90% of the cells within the matrix or on the surface and they coordinate the function of osteoclasts and osteoblasts [10]. Osteoclasts are the cells responsible for bone resorption [9, 11]. They have major role in bone modeling which changes the shape of bone during growth, and bone remodeling which maintains the integrity of adult skeleton [10]. Bone is highly dynamic organ that undergoes significant turnover compared to the other organs in the body. Bone remodeling consists of two main process, bone formation and bone resorption which are tightly coupled. Loss of balance between these will cause diseases such as

osteoporosis, osteopetrosis and osteosclerosis. Complex intracellular signaling pathways are involved in bone metabolism, and regulation of balance between the osteoprogenitor cells, mature osteoblasts, osteocytes and osteoclasts [19].

Each bone cell types has a characteristic gene expression profile, and some genes are specific to each. The selectivity of gene expression allows the use of specific promoters to drive *Cre*-expression (via transgenesis) in particular subtypes of bone cells. For example, dentin matrix protein1 (*DMP1*) is expressed by osteocytes and some late stage osteoblasts. *DMP1* regulates cell attachment and cell differentiation, activates matrix metalloproteinase-9 and affects bio mineralization [12, 13, 4]. In this study, I used the *DMP1-Cre* transgenic mouse which has a DMP1 promoter that drives Cre recombinase expression only to late stage osteoblasts and osteocytes. Therefore these cells would be expected to undergo Cre-mediated recombination.

1.4. *DMP1-Cre* mouse line:

The generation of *DMP1-Cre* mouse has been reported previously [20]. Briefly, the mouse DMP1 promotor used in these experiments was a 14-kb fragment of a full length promotor that contains a 9624- bp promotor region, a 95-bp exon 1, a 4626-bp intron I and a 17-bp initial non coding region of exon II. This fragment was sub cloned into the Xhol site of pMHCre vector which contains the Cre cDNA. The 15.0-kb *DMP1-Cre* transgene was then released from vector backbone with the use of restriction enzyme Pme1 and purified. The transgene

was microinjected into the pronuclei of fertilized mouse eggs isolated from CD-1 outbred mice. The surviving eggs were transferred into oviducts of pseudopregnant CD-1 recipient mice for generation of the transgenic mice [20].

To determine whether the recombination has occurred, I crossed *DMP1-Cre* mouse to a fluorescent Cre-reporter line- *Ai9*.

Ctsk is a gene whose expression is strong in the osteoclast. Cathepsin K (Ctsk) is a cysteine protease upregulated during osteoclastogenesis and is expressed in the mature osteoclast [15]. I used the *Ctsk-Cre* mouse where Ctsk promoter drives Cre recombinase expression, so that presumably only osteoclasts would undergo Cre-mediated recombination.

1.5. *Ctsk-Cre* mouse line:

The generation of *Ctsk-Cre* mouse used in this study has been reported previously [21]. Briefly, the plasmid -pGL3-CK5.0 containing nucleotides 3350 to 1660 of the *Ctsk* gene in a pGL3 vector were modified using standard restriction digestion and cloning techniques to include the Cre coding sequence and generate the *Ctsk-Cre* construct. The *Ctsk-Cre* fragments were excised and separated from the plasmid by restriction digestion and agarose gel electrophoresis. The constructs were purified and microinjected into the pronuclei of fertilized oocytes. Surviving eggs were transferred into pseudopregnant female

mouse. PCR was performed with the tail genomic DNA using primers to confirm the presence of the *Ctsk-Cre* gene [21].

To determine whether the recombination has occurred, I crossed the Cre-expressing mice to the same fluorescent Cre-reporter line—*Ai9*.

1.6. *Ai9* reporter line:

Ai9 is a transgenic Cre reporter mouse line that expresses red fluorescent marker when loxP recombination has occurred. Several Cre mediated studies have been reported in which the *lacZ* gene is turned on in cells by Cre recombinase. The advantage of fluorescent reporter over the conventional the *lacZ* reporting system is that the former does not requires substrate addition step as does the *lacZ* method. Also, the bright fluorescent color can be easily visualized in positive cells. In the *Ai9* fluorescent reporter mouse the ubiquitously expressed Rosa 26 locus is used to express the tomato reporter. The Rosa 26 locus is modified by insertion of a construct containing a ubiquitous CAG promotor, a floxed stop codon followed by the flourophorem tdTomato which encodes a red fluorescent protein (Figure 2). In these mice, the transgene produces no transcript because of the functional (floxed) stop codon that precedes tomato. When Cre is introduced into the cell, Cre recombines the loxP sites that surround the stop sequence deleting the stop so the cell can transcribe the tomato allele [15]. Thus, this mouse “reports” via a bright red signal, the cell in which recombination has occurred. Cells in which no recombination has

occurred do not fluoresce red. Here, the *Ai9* reporter model allows us to test the reliability, cell-specificity, off-target effects, and timing of different Cre mouse models that are used for bone genetic studies in mouse models.

Figure 2 (from reference 15): Schematic diagram of Ai9 construct. It contains a CAG promoter, a floxed stop sequence, the red fluorescent protein tdTomato, Woodchuck hepatitis post-transcriptional regulatory element (WPRE) for high level expression, and other elements such as PA, AttB, Pr, Frt and Neo for plasmid integration and positive cell selection.

To test if the *Ai9* reporter interferes with any genes or other factors in the bone-Cre models to give false positive or false negative results, I tested the Cre-expression of a global Cre-expressing mouse –*E2A-Cre* when recombined with *Ai9*. The *E2A-Cre* carries a Cre transgene under the control of an adenovirus *E2A* promoter, a ubiquitous promoter that can drive Cre- expression in a wide range of tissue/cells in mouse [38]. The *E2A* product is an activator of many B cell specific genes.

1.7. *E2A-Cre* mouse line:

The generation of *E2A-Cre* mice used in this study has been reported previously [25]. Briefly, the *E2A* plasmid was constructed by replacing the human cytomegalovirus promotor in pBS 185 with the adenovirus promoter from *pEII-*

lacZ. This construct was microinjected into mouse zygote for production of transgenic mouse [25].

The Cre mouse models included in this study and their cell type targets are listed in Table 1.

Cre mouse lines	**Targeted Tissue/cell**
DMP1-Cre	Osteoblast and osteocytes
Ctsk-Cre	Osteoclast
E2A-Cre	All cell type/tissue type

Table 1: Cre mouse lines used in this study.

Ai9 mouse line was crossbred with all the above listed '*bone –Cre'* lines. Double positive offspring were selected by molecular biology methods for further studies. To study Cre-mediated recombination in bone and other tissues of the mice, I applied various histological methods and fluorescent microscopic analysis.

2. Research Methods

2.1. Generation of mice that harbor *Ai9* transgene, and *Cre* transgene:

The *Ai9* reporter mouse line, B6.Cg-*Gt (ROSA) 26Sortm9* $^{(CAG\text{-}tdTomato)}$ /J strain was purchased from 'the Jackson laboratory'. The *DMP1-Cre* transgenic mouse line was a gift from Jerry Feng [20]. The *Ctsk-Cre* transgenic mouse line was a gift from W S M Chiu [21]. The *E2A-Cre* transgenic mouse line was also a commercial line purchased from 'the Jackson laboratory'.

Homozygous *Ai9* male (Male mice are homozygous for *Ai9* gene) mice were mated with hemizygous *E2A-Cre*, *DMP1-Cre* and, *Ctsk-Cre* mice to obtain *Ai9* positive mice that were positive or negative for Cre. PCR was performed to select the *Ai9* and different *Cre* double positive mice. Three mice samples of 4-6 weeks old from each *Cre* lines were studied during the time period of June 2013-October 2014. The mice samples included both males and females.

2.2. DNA extraction and PCR:

Samples of ear tissue from mice were used to extract DNA. Ear notching was also helpful to tag, identify and differentiate mice in each cage. Animals in each cage were ear punched using an ear punch device and the ear pieces were collected using forceps. The ear notching tools were cleaned after handling each mice using 70% alcohol solution. Mice were differentiated as right front (RF),

right rear (RR), left front (LF) and left rear (LR) based on where the ear was notched.

PCR was performed using HotSHOT (Hot Sodium Hydroxide and Tris) reagents. HotSHOT lysis reagent is an alkaline solution (pH 12) prepared with 25 mM NaOH and 0.2 mM disodium EDTA. The solution was prepared by dissolving the salt in water without adjusting the pH. HotSHOT neutralization reagent is 40mM Tris-HCl with a pH 5, and was prepared by dissolving Tris-HCl in water without adjusting the pH. The ear tissue samples were collected in thermal cycler strip tubes. 75uL of the alkaline lysis reagent was added to the tubes and heated to 95ºC for 10 minutes to 1 hour and then cooled to 4ºC in the PCR cycler. 75 uL neutralizing reagent was added to each sample tubes immediately. 3 uL of the DNA sample was added to 12 uL of the PCR mixture. PCR mixture has 7.5 uL of RED PCR mix, 0.35 uL of each primers (20uM stock), and 3.45 uL of PCR grade water (Promega, Madison, WI, USA). The tubes were placed in PCR cycler for the following thermo cycling procedure: Reactions were held at 94ºC for 3 minutes for initial denaturing, 30 seconds for denaturing, 60ºC for 30 seconds for annealing, 72ºC for 1 minute for extension (35 cycles of denaturing, annealing and extension) and at 72ºC for another 10 minutes for final extension. Tubes were held at 4ºC for 40 cycles at 95ºC for 40 seconds and 60ºC for 45 seconds. Following amplification, 7-10uL of the PCR product was added to each well of a 2.2% agarose gel placed horizontally in an electrophoresis chamber. TAE (0.5X0 was used as the loading buffer. Electrophoresis was performed at 100 V for 45

minutes in 1X TBE buffer (89mM Tris/89mM boric acid, 2mM EDTA). Gels were imaged under the UV light trans-illuminator and images were taken [33].

2.2.1. PCR to test *Ai9* positive mouse:

DNA extract was added into PCR mix solution containing master mix, DNase free water and the 4 Primers, **1**. oIMR9020: 5'- AAG GGA GCT GCA GTG GAG TA – 3', **2**. oIMR9021: 5'- CCG AAA ATC TGT GGG AAG TC, **3.** oIMR9103: 5'- GGC ATT AAA GCA GCG TAT CC- 3', **4.** oIMR9105: 5'- CTG TTC CTG TAC GGC ATG G- 3'. PCR products were analyzed for positive *Ai9* transgene of band size 196 bp, and the control *Rosa-26* gene of 297 bp by running agarose gel electrophoresis at 100V for 45 minutes.

2.2.2. PCR to test *DMP1-Cre* positive mouse:

Using ear tissue sample from the mice, DNA was extracted by the same method described in method 2.2. As described in method 2.2.1, PCR was performed but using different primers, **1.** 5'-CCG GGC TGC CAC GAC CAA GT – 3', **2.** 5'- GCG CGAGTT GAT AGC TGG CTG GT -3', **3.** 5'-AAA GTC GCT CTG AGT TGT TAT -3', **4.** GGA GCG GGA GAA ATG GAT ATG. Primers 1 and 2 are for *DMP1-Cre* forward and reverse sequence, and 3 and 4 are for internal control *Connexin-43* wild type forward and reverse. PCR products were analyzed for positive *DMP1-Cre* gene of band size 529bp and the *Connexin-43* of 1000bp by running agarose gel electrophoresis at 100V for 45 minutes.

2.2.3. PCR to test *Ctsk-Cre* positive mouse:

DNA was extracted from the ear notch sample applying the same procedure given in method 2.2. PCR was performed as described in method 2.2.1, but different set of primers, **1.** 5'- GAG TGA TGA GGT TCG CAA GA-3', **2.** 5' CTA CAC CAG AGA CGGAAATC-3', **3**.5'-TCATGCCCGGCACAAGTGAGAC-3, **4**.5'TCACCCCAAGCTGACTCAACCG-3'. 1 and 2 are primers for *Ctsk-Cre* forward and reverse, and 3 and 4 are for internal control *connexin-43* forward and reverse sequence. PCR products were analyzed for a 600 bp *Ctsk-Cre* band and 1000 bp *Connexin-43* band by running agarose gel electrophoresis at 100V for 45 minutes.

2.2.4. PCR to test *E2A-Cre* positive mouse:

DNA was extracted from ear notch samples by the same procedure described in method 2.2. PCR was performed with the extracted DNA sample by following the procedure in method 2.2.1, but using different set of primers. **1**. oIMR1084: 5'- GCG GTC TGG CAG TAA AAA CTA TC – 3', **2**. oIMR1085: 5'- GTG AAA CAG CAT TGC TGT CAC TT- 3', **3**. oIMR7338: 5'- CTA GGC CAC AGA ATT GAA AGA TCT – 3', **4**. oIMR7339: 5'- GTA GGT GGA AAT TCT AGC ATC ATC C – 3'. Primers 1 and 2 are for *E2A-Cre* transgene forward and reverse, and 3 and 4 are for forward and reverse band of internal control *IL-2* gene. PCR products were analyzed for 100bp *E2A-Cre* transgene band and 324 bp *IL-2* internal control band by running agarose gel electrophoresis at 100V for 45 minutes

2.3. Perfusion and collection of organs from mice:

The *Ai9, Cre* - double positive mice were subjected to anesthesia by giving isoflurane inhalation. The pinch-response method was used to confirm that the animal was under deep anesthesia. An incision was made with scalpel through the abdomen along the length of diaphragm. With sharp scissors the body was cut through the connective tissue at the bottom of the diaphragm to reach the rib cage. The thoracic cavity was clamped open with a chest retractor to expose the heart. The heart was held steady with forceps, and needle was inserted into protrusion of left ventricle straight up about 5mm. 4% PBF solution was perfused into the organs. The body was cut open and femur bones and different organs such as liver, kidney, spleen, duodenum, heart and brain were collected in 4% PBF.

2.4. Freeze-embedding of the sample:

The femur bone and the other different tissue samples were rapidly frozen in -72ºC cold N-Hexane in order to minimize freezing artifacts. Each of the freshly frozen samples (positive and negative) were placed in a rectangle shaped stainless steel container filled with OCT. The OCT containing tissue samples were completely frozen by keeping the metal block in the cold N- Hexane. The frozen block was stored at -80ºC until further analysis.

2.5. Cryosectioning:

The frozen OCT block was fixed to a circular disc with OCT gel and then placed on the stage of a cryomicrotome. The block was trimmed to expose the tissue to the surface of block. The adhesive film purchased from Japan [18] was cut so as to have the same width of the block and was adhered to the cutting surface of the block. 5 µm thick sections were collected on the adhesive film by cutting the block along with the film slowly at a constant speed. Two contiguous sections were collected, one for fluorescent cell analysis and the other for stained cell analysis [18].

2.6. Staining of the tissue:

The film containing tissue sample was washed immediately in absolute alcohol followed by water to remove the OCT. For fluorescent analysis, the tissue was stained with a DAPI solution (7ul in 15ml of water) for 2 minutes. The second section was stained with 0.1% toluidine blue for 30 seconds for light microscopic analysis. Excess stain was removed with water. The tissue sections were mounted by placing the section side of the adhesive film on a glass slide coated with SCMM mounting medium. The excess mounting media was carefully wiped off using a filter paper.

2.7. Microscopic analysis:

For analyzing fluorescent expression, the tissue sections were observed under fluorescent microscope using a filter for Texas Red by means of a program

‘Osteomeasure’. The cells were observed at 20X magnification and images of different fields of each sample were captured and saved. The same field of each fluorescent picture was found in the stained section under white light to match and sort cells, and the images were captured. Images of all different bone tissues and soft tissues (both positive and negative) were taken in this manner.

2.8. Measuring the Cre-expression:

In order to study whether there is significant Cre-expression in each tissue of the mice, the percentage of positive fluorescent cell was calculated by measuring the number of positive red fluorescent cells over the total number of cells (DAPI-stained nuclei) in the tissues. The total number of cells from each tissue sample was counted by ImageJ-automated counting software tool and the red positive cells were counted manually. Tissue samples from three different *DMP1-Cre* and *Ctsk-Cre* mice were analyzed for fluorescent mediated Cre recombinase expression. Standard deviation was calculated from the average of the percentage of positive Cre-expressed cells from the three mice.

2.9. Cell counting using ImageJ:

ImageJ is a public domain Java image processing and analyzing program. It can be used to calculate area and pixel value statistics of images of user defined selections. There are vast repertoire of plugins available that extend ImageJ’s functionality beyond its basic core to make it a powerful program. ImageJ

provides a cost effective and reliable way to count fluorescent labelled cells. It is a free software which can be downloaded from internet [34, 37].

2.10. Automated counting of entire cells in an image:

Since there are large number of cells present in each field of the tissue sections manual counting is not practical. Automated counting was adapted to count the DAPI stained nuclei of entire cells present in different fields of soft tissue that don't require additional plugin. The image to be counted was opened in the ImageJ software. The colored image was converted to grey scale by selecting Image-> Type-> 8-bit to convert grey scale. Once the image was in grey scale, Image-> Adjust-> Threshold, was used to highlight all the cells to be counted. The sliders were used to highlight the cells. Some nuclei were merged together. To cut them apart, Process-> Binary-> Watershed was used. Once the binary image of the particle was ready, Analyze-> Analyze particle was used [35].

2.11. Counting cells in a region of interest:

To count the cells in different regions of bone tissue (marrow, matrix) separately, an ITCN (Image-based Tool for Counting Nuclei) plugin of ImageJ which enables the count of nuclei in a selected region of interest was adopted. Here the inputs were: (1) an estimation of diameter of a nucleus, (2) an estimation of the minimum distance between nuclei and (3) the region of interest selected with ImageJ's area selection tool. ITCN plugin version 1.6 was downloaded for this purpose. The image was opened in 'ImageJ', converted to 8-bit. The ITCN plugin

was opened and the width was entered into the text field. The width is the approximate diameter of the cells to be counted and its value was determined using the selection tool to draw a line that is the diameter of a cell, and pressing the adjacent ‘Measure line length’. The minimum distance was entered into the text field. The minimum distance is the approximation of the distance between nuclei centers. Its value was also determined using the line selection tool and pressing ‘Measure line length’. The threshold was entered into text field or using adjacent slide bar. The threshold determines the quality of detected cells. A region of interest was selected using ImageJ selection tool, and ‘count’ was used [36].

3. Results

3.1. PCR result showing the presence of *Ai9* transgene:

PCR was performed with ear tissue samples to detect the presence of *Ai9* transgene in the offspring of the *Ai9* positive male and different *Cre* positive female breeders, using respective primers. The gel was analyzed for the presence of 196 bp band of *Ai9* transgene and 297bp *Rosa26* band of internal control wild type *Ai9* gene. Figure 3 shows PCR followed by agarose gel electrophoresis from *Ai9* mice tissue.

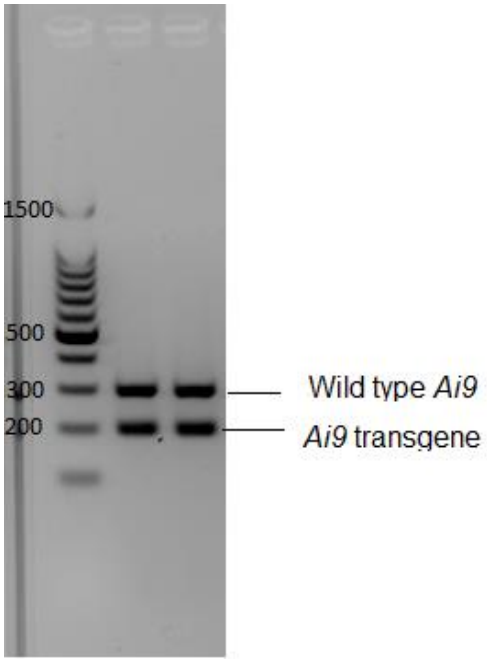

Figure 3: Agarose gel showing the Ai9 band. The first lane shows the DNA ladder. The second and third lanes show 2 bands. The high band that aligns with 300 bp is the wild type *Ai9* (*Rosa-26*) and the low band that aligns with 200 bp is *Ai9* transgene.

3.2. PCR results showing the presence of *E2A–Cre* transgene:

PCR was performed with ear tissue samples to detect the presence of *E2A-Cre* transgene in the offspring of the *Ai9* positive male and *E2A-Cre* positive female breeders, using respective primers. The gel was analyzed for the presence of 100 bp band of *E2A-Cre* transgene and 324bp band of internal control *IL-2*. Figure 4 shows PCR followed by agarose gel electrophoresis from *E2A-Cre* mice tissues.

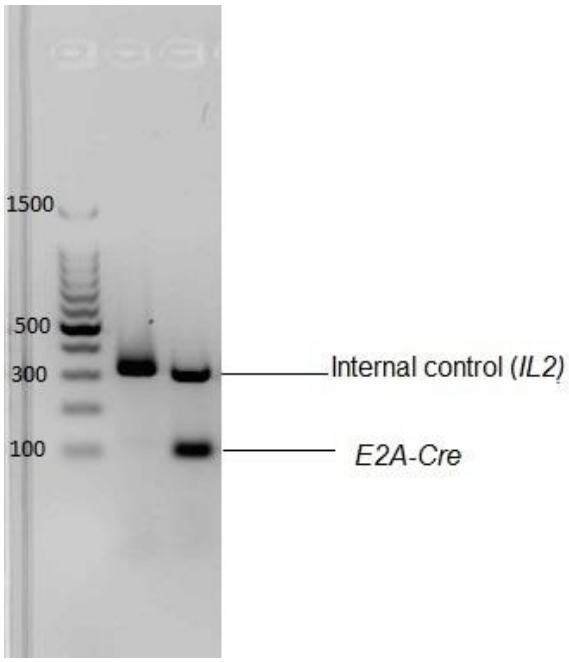

Figure 4: Agarose gel showing the *E2A-Cre* band. The first lane shows the DNA ladder. The second lane is a negative sample which shows only internal control band *IL2* that aligns with 300bp band of the ladder. The third lane shows 2 bands. The high band that aligns with 300 bp band of the ladder is the internal control *IL-2* and the low band that aligns with 100 bp is *E2A-Cre* transgene.

3.3. Fluorescent microscopic and qualitative analysis results of the bone tissues from the *E2A-Cre* mice:

To determine if there is Cre-mediated recombination in the bone tissue of *E2A-Cre* mouse line, the *Ai9* mice were crossbred to the *E2A-Cre* mice. The double positive (*Ai9+/E2A-Cre+*) offspring were perfused and 5 um thick sections of the femur bone tissue were prepared for histological analysis. The bone tissue sections were stained with DAPI. Figure 5 shows the fluorescent microscopic images (left) and toluidine blue stained white light images (right) of bone tissue from an *E2A-Cre* positive mouse. Figure 6 shows bone tissue from an *E2A-Cre* mouse without DAPI nuclear staining. Figure 7 shows the picture of bone tissue from a negative *E2A-Cre* mouse. The skeletal muscle, osteoclast, osteoblast and majority of the osteocytes show red fluorescent signal which indicates the presence of *Cre* recombinase in these tissues. However the marrow cells show no red fluorescence which indicates that *Ai9* is not reporting fluorescence in the bone marrow. The results show that *Ai9* is successful as a Cre reporter line in bone. Since it represses fluorescence in bone marrow of *E2A-Cre* mouse line, it is unlikely that we will be able to determine if there is Cre-mediated recombination happening in this compartment in the bone-Cre mouse models.

Fluorescence White light (toluidine blue)

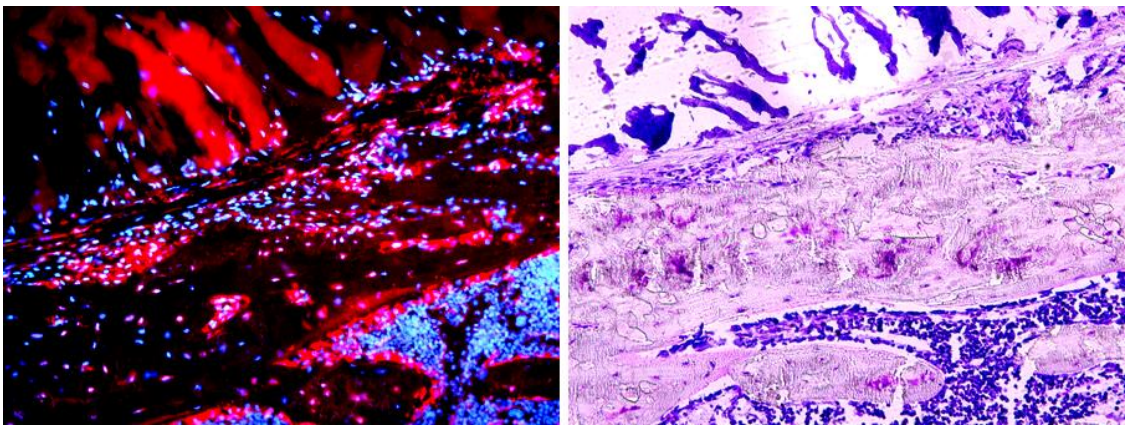

Figure 5: Microscopic images of bone tissue from an *E2A-Cre* positive mouse (DAPI stained). Fluorescent (left) and toluidine blue stained (right) images of bone tissue with muscle and marrow from an *E2A-Cre* positive mouse. The fluorescent image shows red fluorescence in muscle, and bone cells such as osteocytes, osteoblasts and osteoclast. The marrow shows blue color with DAPI staining. The toluidine blue stained image shows the marrow, bone matrix and muscle in purple color.

Fluorescence White light (toluidine blue)

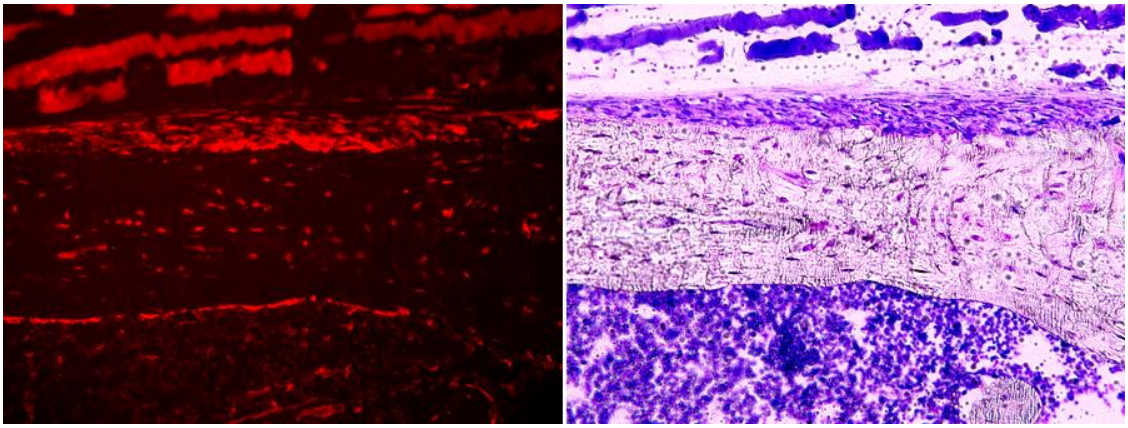

Figure 6: Microscopic images of bone tissue from an *E2A-Cre* positive mouse (without DAPI). Fluorescent (left) and toluidine blue stained (right) images of bone tissue with muscle and marrow from an *E2A-Cre* positive mouse. The fluorescent image shows red fluorescence in muscle and bone cells such as osteocytes, osteoblasts and osteoclast. The toluidine blue stained image shows the marrow, bone matrix and muscle in purple color.

Fluorescence White light (toluidine blue)

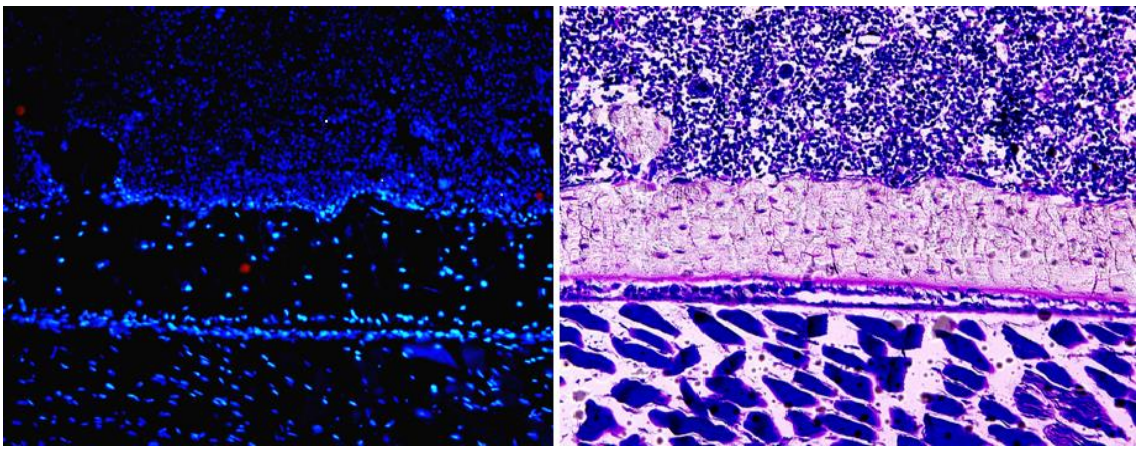

Figure 7: Microscopic images of bone tissue from an *E2A-Cre* negative mouse. Fluorescent (left) and toluidine blue stained (right) images of bone tissue with muscle and marrow from an *E2A-Cre* negative mouse. In the fluorescent image, the cell nuclei show blue color with DAPI staining. The toluidine blue stained image shows the marrow, bone matrix and muscle in purple color.

3.4. Fluorescent microscopic analysis and qualitative results of the soft organs/ tissues from the *E2A-Cre* mice:

To determine if there is Cre-mediated recombination in the soft tissues of *E2A-Cre* mouse line, the *Ai9* mice were crossed to the *E2A-Cre* mice. The double positive (*Ai9+/E2A-Cre+*) offspring were perfused and 5 um thick sections of soft tissues were prepared for histological analysis. The tissue sections were stained with DAPI. Figure 8-19 show the fluorescent (left) and toluidine blue stained (right) microscopic analysis results of both positive and negative soft tissues from the *E2A-Cre* mice. The *E2A-Cre* positive mice show significantly strong red fluorescence in majority of the cells in the tested soft tissues such as heart, kidney, liver, brain, duodenum and spleen. The negative control mice show no red fluorescent in any of the tissues. The nuclei appear as blue color with DAPI

staining. The results indicate that *Ai9* mouse is successful as a reporter line to study Cre-mediate recombination in all the tested soft tissues.

Fluorescence White light (toluidine blue)

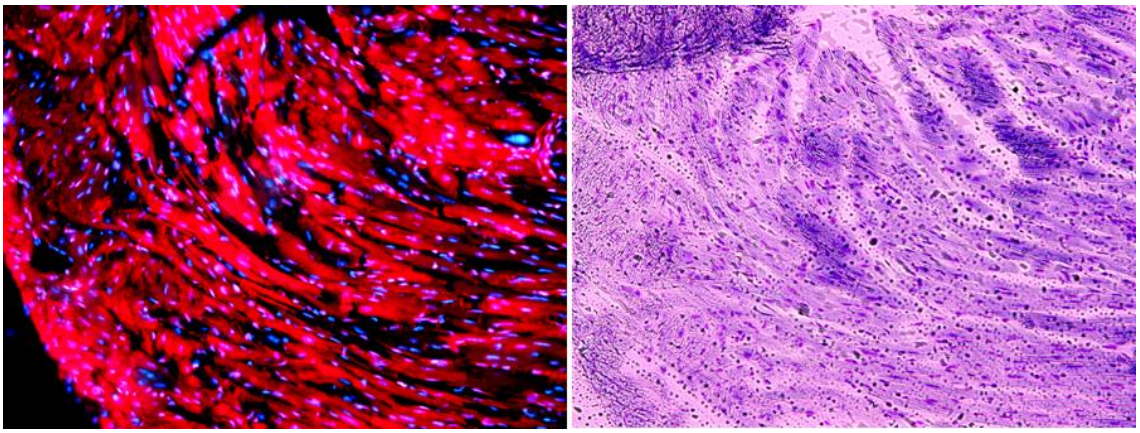

Figure 8: Microscopic images of heart tissue from an *E2A-Cre* positive mouse. Fluorescent (left) and toluidine blue stained (right) images of heart tissue from an *E2A-Cre* positive mouse. In the fluorescent image, the heart cells appear as red color with Cre-expression and the nuclei as blue with DAPI staining. The cells appear in purple color in the toluidine blue stained image.

Fluorescence White light (toluidine blue)

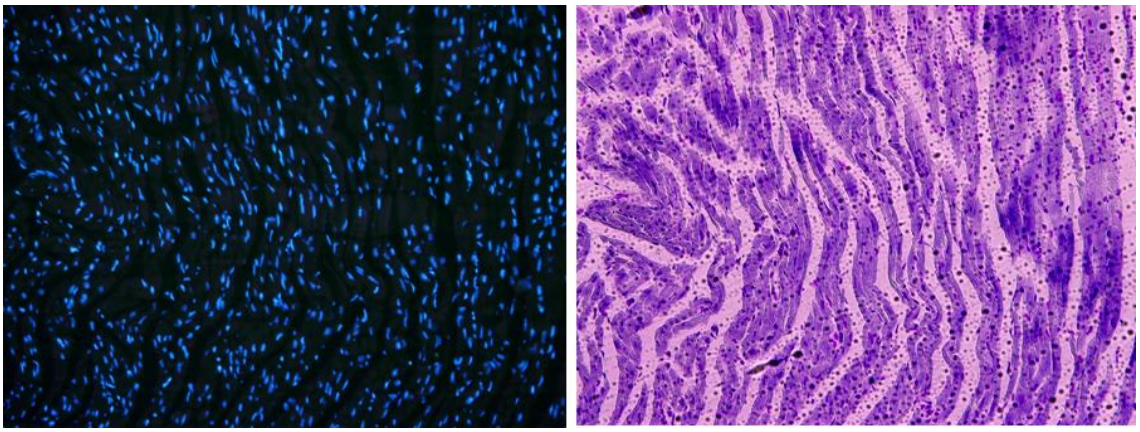

Figure 9: Microscopic images of heart tissue from an *E2A-Cre* negative mouse. Fluorescent (left) and toluidine blue stained (right) images of heart tissue from an *E2A-Cre* negative mouse. The blue color in the fluorescent image is nuclei with DAPI staining. The cells appear in purple color the toluidine blue stained image.

Fluorescence White light (toluidine blue)

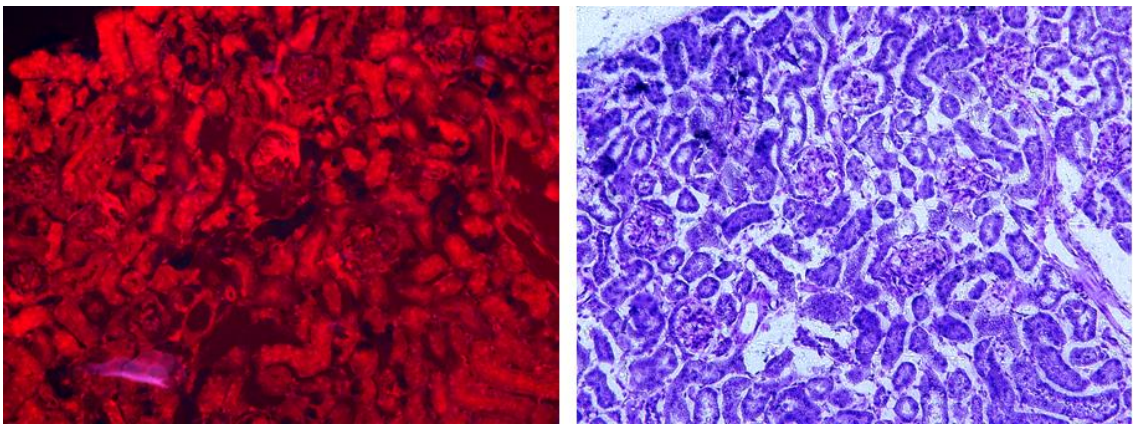

Figure 10: Microscopic images of kidney tissue from an *E2A-Cre* positive mouse. Fluorescent (left) and toluidine blue stained (right) images of kidney tissue from an *E2A-Cre* positive mouse. In the fluorescent image, the kidney cells show red color with Cre-expression and the nuclei appears as blue with DAPI staining. The cells appear in purple color in the toluidine blue stained image.

Fluorescence White light (toluidine blue)

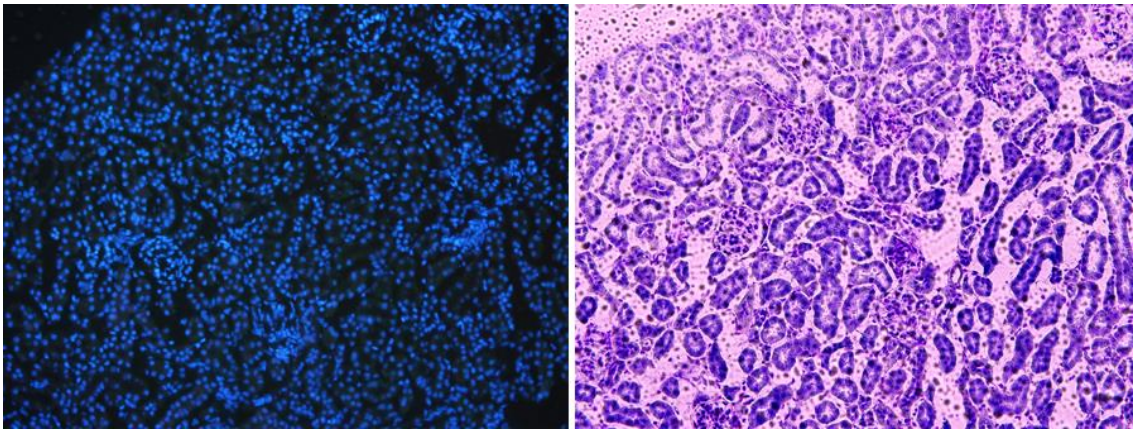

Figure 11: Microscopic images of kidney tissue from an *E2A-Cre* negative mouse. Fluorescent (left) and toluidine blue stained (right) images of kidney tissue from an *E2A-Cre* negative mouse. The blue color in the fluorescent image is nuclei with DAPI staining. The cells appear in purple color in the toluidine blue stained image.

Fluorescence White light (toluidine blue)

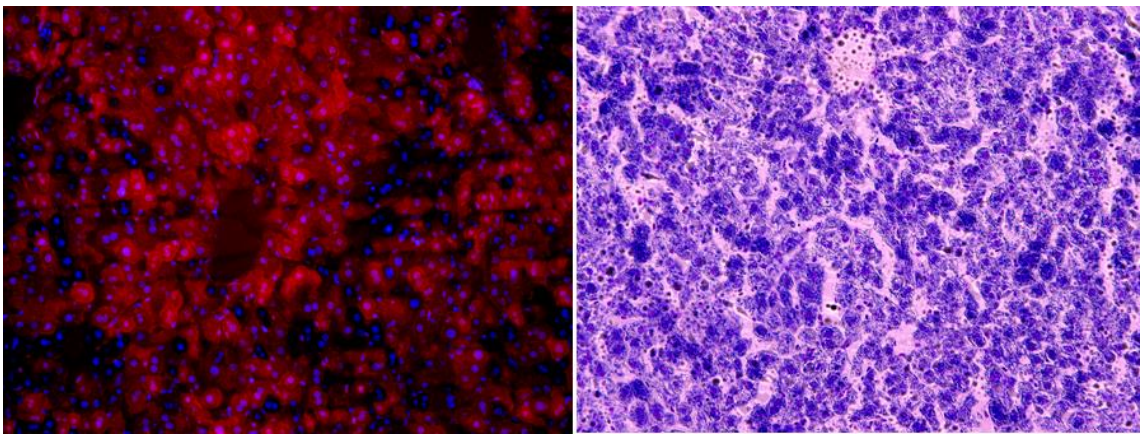

Figure 12: Microscopic images of liver tissue from an *E2A-Cre* positive mouse. Fluorescent (left) and toluidine blue stained (right) images of liver tissue from an *E2A-Cre* positive mouse. In the fluorescent image, the liver cells show red color with Cre expression and the nuclei appear as blue with DAPI staining. The cells appear in purple color in the toluidine blue stained image.

Fluorescence White light (toluidine blue)

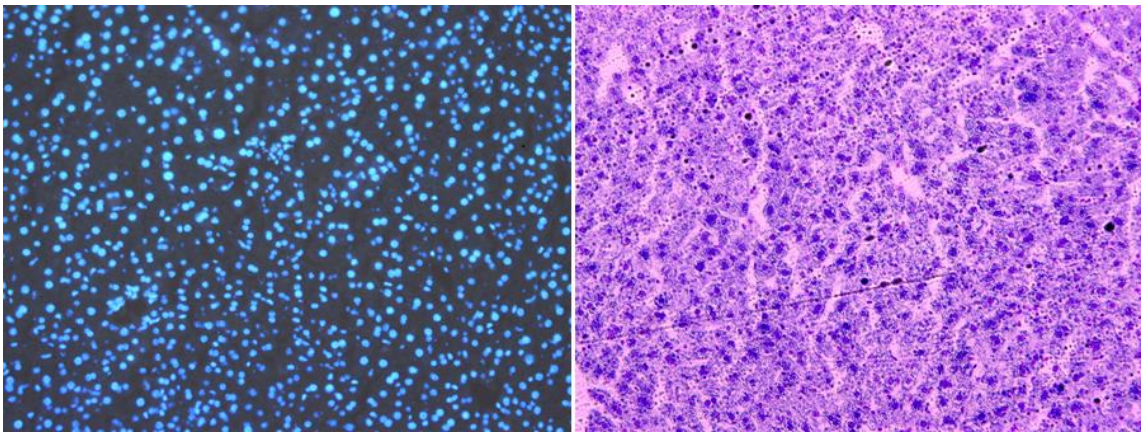

Figure 13: Microscopic images of liver tissue from an *E2A-Cre* negative mouse. Fluorescent (left) and toluidine blue stained (right) images of liver tissue from an *E2A-Cre* negative mouse. The blue color in the fluorescent image is nuclei with DAPI staining. The cells appear in purple color in the toluidine blue stained image.

Fluorescence White light (toluidine blue)

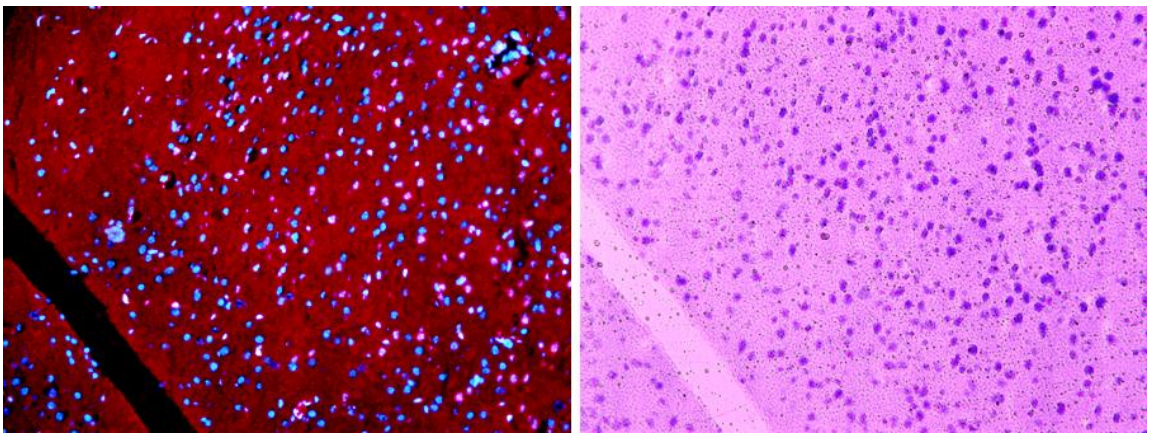

Figure 14: Microscopic images of brain tissue from an *E2A-Cre* positive mouse.
Fluorescent (left) and toluidine blue stained (right) images of brain tissue from an *E2A-Cre* positive mouse. In the fluorescent image, the brain cells show red color with Cre-expression and the nuclei appear as blue with DAPI staining. The cells appear in purple color in the toluidine blue stained image.

Fluorescence white light (toluidine blue)

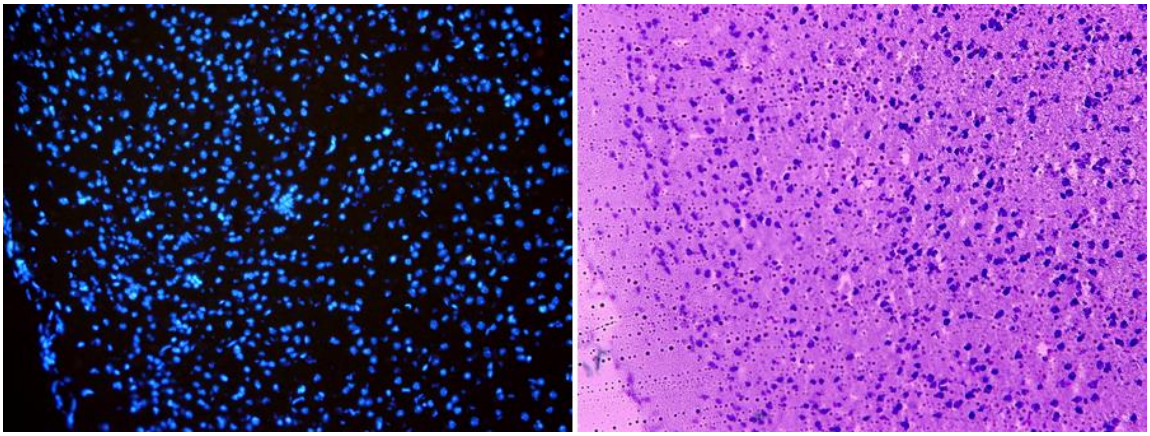

Figure 15: Microscopic images of brain tissue from an *E2A-Cre* negative mouse.
Fluorescent (left) and toluidine blue stained (right) images of heart tissue from an *E2A-Cre* negative mouse. The blue color in the fluorescent image is nuclei with DAPI staining. The cells appear in purple color in the toluidine blue stained image.

Fluorescence White light (toluidine blue)

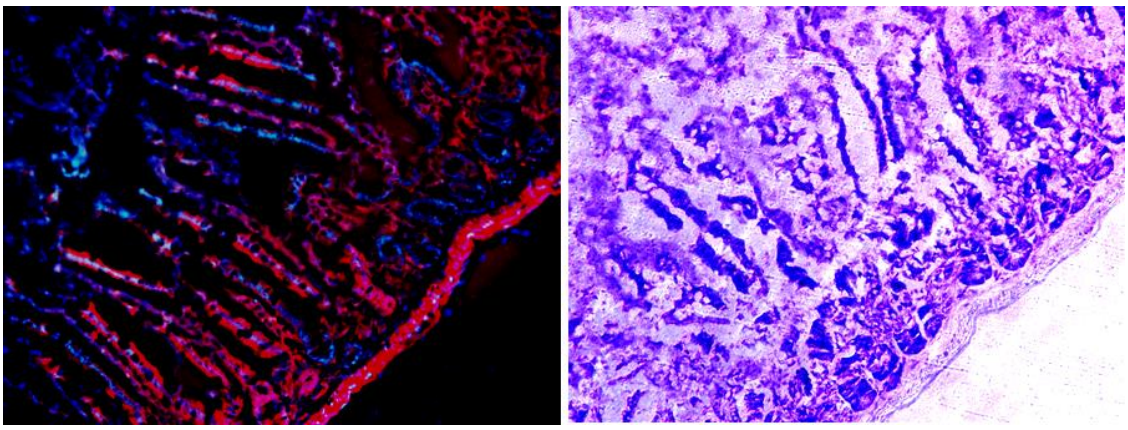

Figure 16: Microscopic images of duodenum tissue from an *E2A-Cre* positive mouse. Fluorescent (left) and toluidine blue stained (right) images of duodenum tissue from an *E2A-Cre* positive mouse. In the fluorescent image, the cells show red color with Cre expression and the nuclei appear as blue with DAPI staining. The cells appear in purple color in the toluidine blue stained image.

Fluorescence White light (toluidine blue)

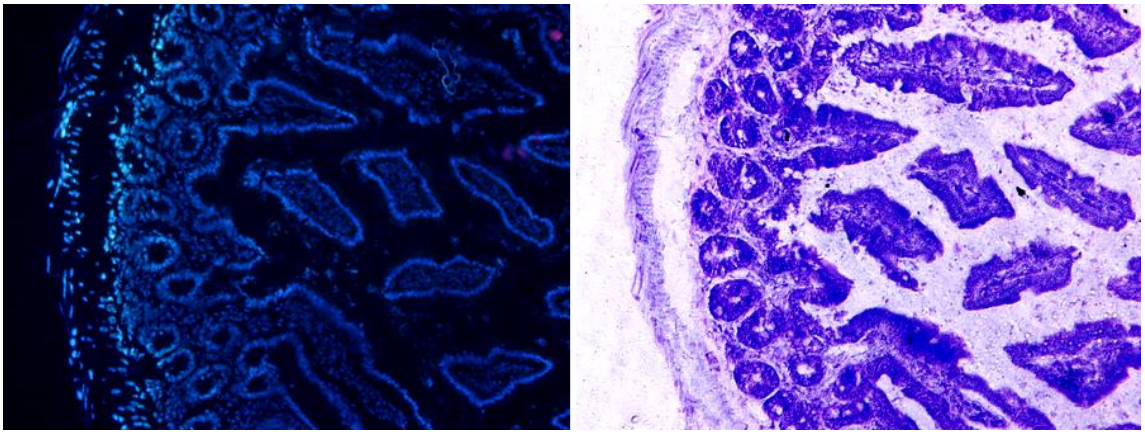

Figure 17: Microscopic images of duodenum tissue from an *E2A-Cre* negative mouse. Fluorescent (left) and toluidine blue stained (right) images of duodenum tissue from an *E2A-Cre* negative mouse. Blue color in the fluorescent image is nuclei with DAPI staining. The cells appear in purple color in the toluidine blue stained image.

Fluorescence White light (toluidine blue)

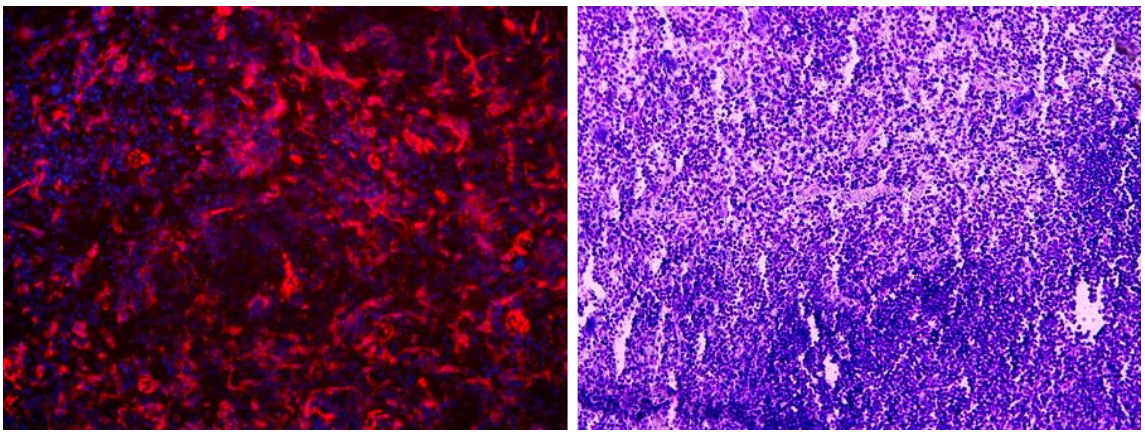

Figure 18: Microscopic images of spleen tissue from an *E2A-Cre* positive mouse. Fluorescent (left) and toluidine blue stained (right) images of spleen tissue from an *E2A-Cre* positive mouse. In the fluorescent image, the spleen cells show red color with Cre expression and the nuclei appear as blue with DAPI staining. The cells appear in purple color in the toluidine blue stained image.

Fluorescence White light (toluidine blue)

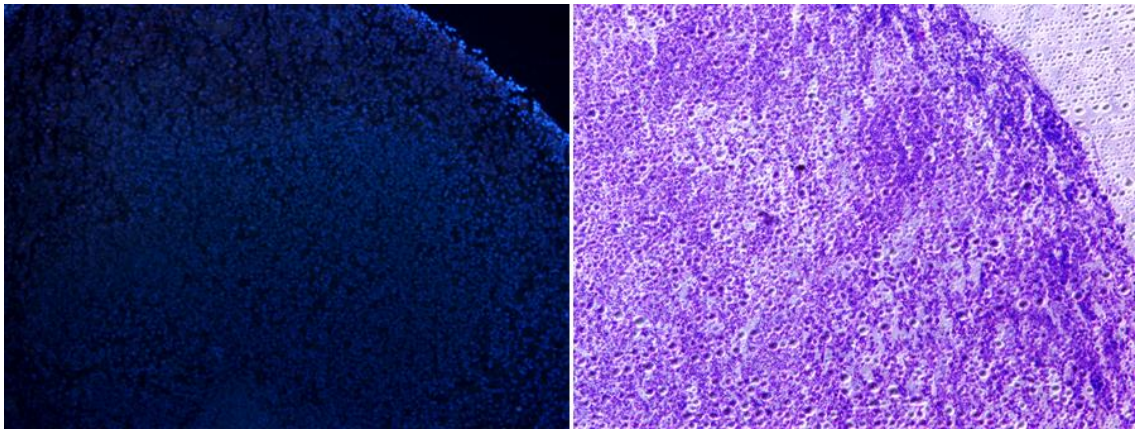

Figure 19: Microscopic images of spleen tissue from an *E2A-Cre* negative mouse. Fluorescent (left) and toluidine blue stained (right) images of spleen tissue from an *E2A-Cre* negative mouse. The blue color in the fluorescent image is nuclei with DAPI staining. The cells appear in purple color in the toluidine blue stained image.

3.5. PCR result indicating the presence of *DMP1-Cre* transgene:

PCR was performed with ear tissue samples from the offspring of the breeders - *DMP1-Cre* female and *Ai9* male to detect the presence of *DMP1-Cre* transgene, using the respective primers. The gel was analyzed for the presence of 529 bp band of *DMP1-Cre* transgene and 1000bp band of *connexin-43* internal control. Figure 20 shows PCR followed by agarose gel electrophoresis from *DMP1-Cre* mice tissue.

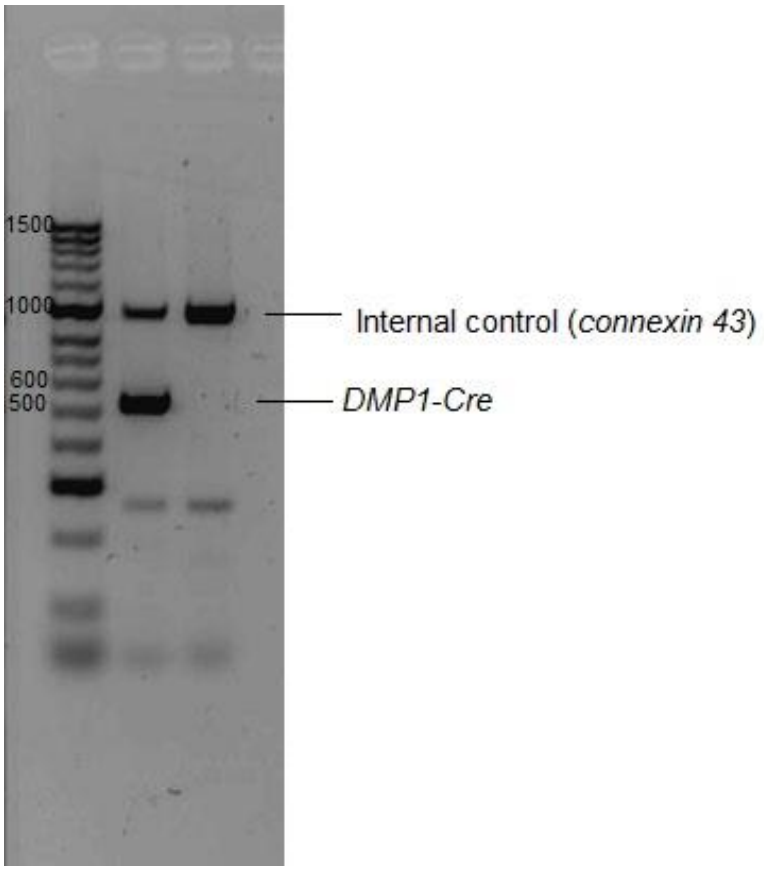

Figure 20: Agarose gel showing the *DMP1-Cre* band. The first lane shows the DNA ladder. The second lane is a positive sample which shows 2 bands. The high band is internal control *Connexin-43* that aligns with 1000bp band of the ladder and the low band is *DMP1-Cre* that align with 500bp band of the ladder. The third lane shows a negative sample which has only the internal control *Connexin-43* band that aligns with 1000 bp band of the ladder.

3.6. Fluorescent microscopic and qualitative analysis results of the bone tissues from the *DMP1-Cre* mice:

To determine if there is Cre-mediated recombination in the bone tissue of *DMP1-Cre* mouse line, the *Ai9* mice were crossed to the *DMP1-Cre* mice. The double positive (*Ai9+/DMP1-Cre+*) offspring were perfused and 5 um thick sections of the femur bone tissue were prepared for histological analysis. The bone tissue sections were stained with DAPI. Images 21a and 21b show fluorescent microscopic images (left) and toluidine blue stained white light images (right) of bone tissue from a *DMP1-Cre* positive mouse. The fluorescent images show bright red fluorescence in the osteocytes, and osteoblast residing in the newly forming bones. The skeletal muscle also shows strong red fluorescence in majority of their cells. Images 22a, 22b and 22c show fluorescent (left) and toluidine blue stained (right) images of the bone tissues from the *DMP1-Cre* positive mice without DAPI nuclear staining. The images show red fluorescence in osteocytes and osteoblasts. In addition, the muscle tissue shows strong red fluorescent expression. Image 23 shows the fluorescent and white light images of bone tissue from *DMP1-Cre* negative control mouse. There is no red fluorescence in *DMP1-Cre* negative mouse and the nuclei is visible as blue color with DAPI staining.

Fluorescent White light (toluidine blue)

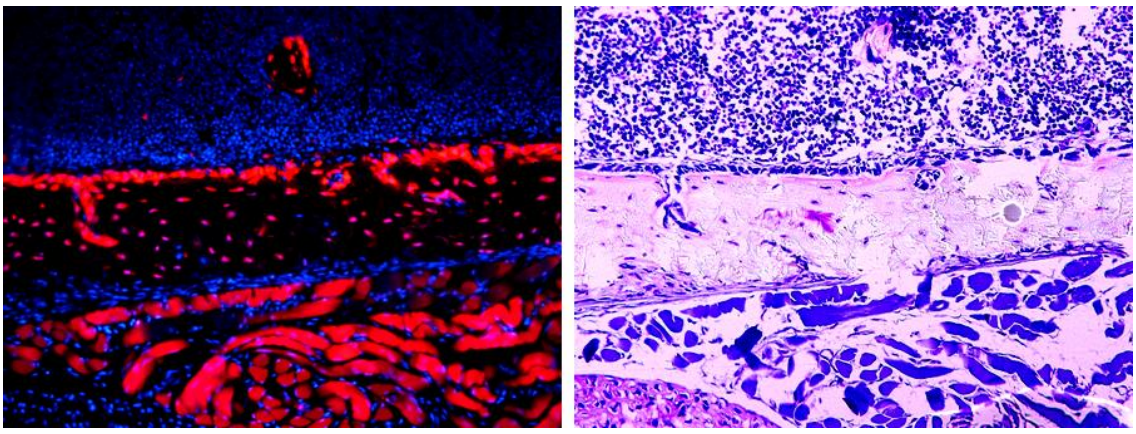

Figure 21a: Microscopic images of bone tissue from a *DMP1-Cre* positive mouse (DAPI stained). Fluorescent (left) and toluidine blue stained (right) images of a bone tissue with muscle and marrow from a *DMP1-Cre* positive mouse. The fluorescent image shows red fluorescence in the muscle and osteocytes. The osteoblasts show red color in the newly forming bone located in the marrow. The marrow shows blue color with DAPI staining. The toluidine blue stained image shows the marrow, bone cells and muscle in purple color.

Fluorescence White light (toluidine blue)

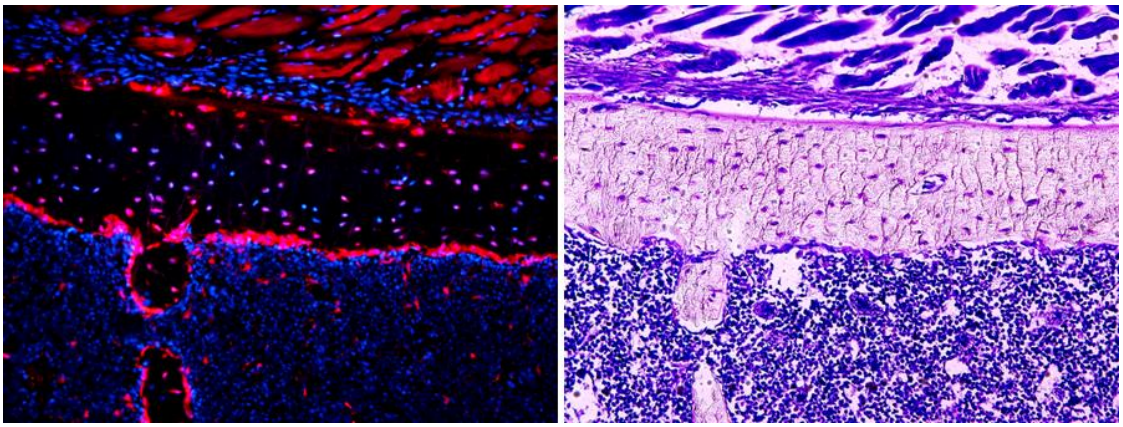

Figure 21b: Microscopic images of bone tissue from a *DMP1-Cre* positive mouse (DAPI stained). Fluorescent (left) and toluidine blue stained (right) images of a bone tissue with muscle and marrow from a *DMP1-Cre* positive mouse. The fluorescent image shows red fluorescence in the muscle cells, osteoblasts and osteocytes. The osteoblasts show red color in the newly forming bone tissue located in marrow. The marrow shows blue colored DAPI stained nuclei and a few Cre positive red cells. The toluidine blue stained image shows the marrow, bone cells and muscle in purple color.

Fluorescence White light (toluidine blue)

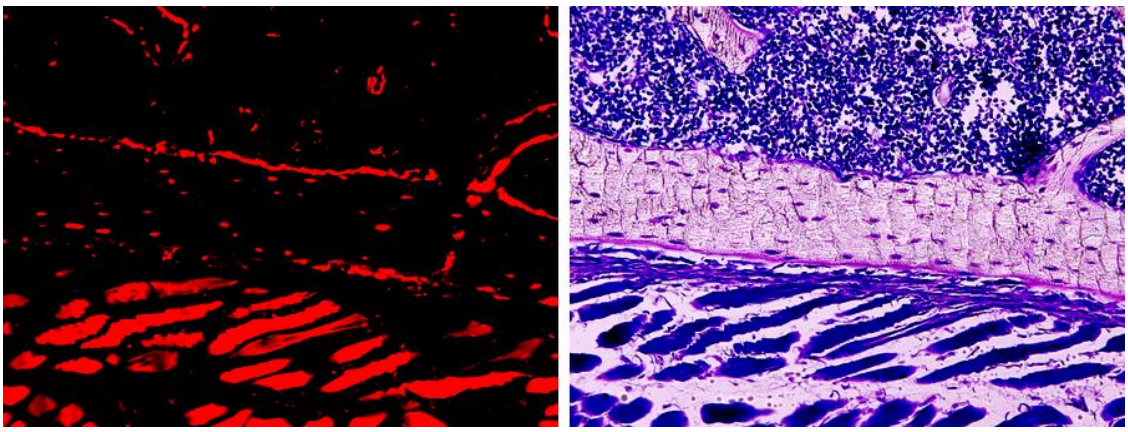

Figure 22a: Microscopic images of bone tissue from a *DMP1-Cre* positive mouse (without DAPI). Fluorescent (left) and toluidine blue stained (right) images of a bone tissue with muscle and marrow from a *DMP1-Cre* positive mouse. The fluorescent image shows red fluorescence in the muscle cells, osteoblasts and osteocytes. The osteoblasts show red color in the newly forming bone tissue located in the marrow. The marrow shows a few Cre positive red cells. The toluidine blue stained image shows the marrow, bone matrix and muscle in purple color.

Fluorescence White light (toluidine blue)

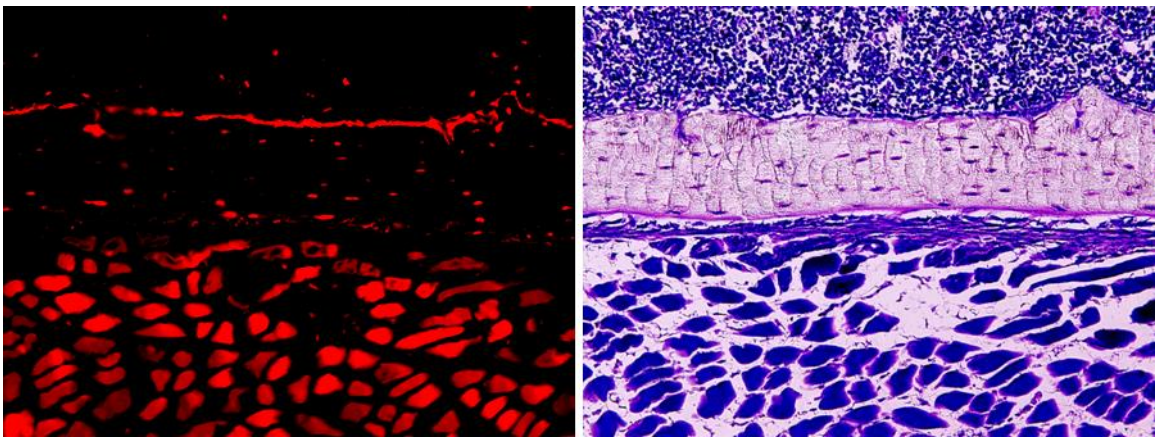

Figure 22b: Microscopic images of bone tissue from a *DMP1-Cre* positive mouse (without DAPI). Fluorescent (left) and toluidine blue stained (right) images of a bone tissue with muscle and marrow from a *DMP1-Cre* positive mouse. The fluorescent image shows red fluorescence in the muscle cells, osteoblasts and osteocytes. The marrow shows a few Cre positive red cells. The toluidine blue stained image shows the marrow, bone cells and muscle in purple color.

Fluorescence White light (toluidine blue)

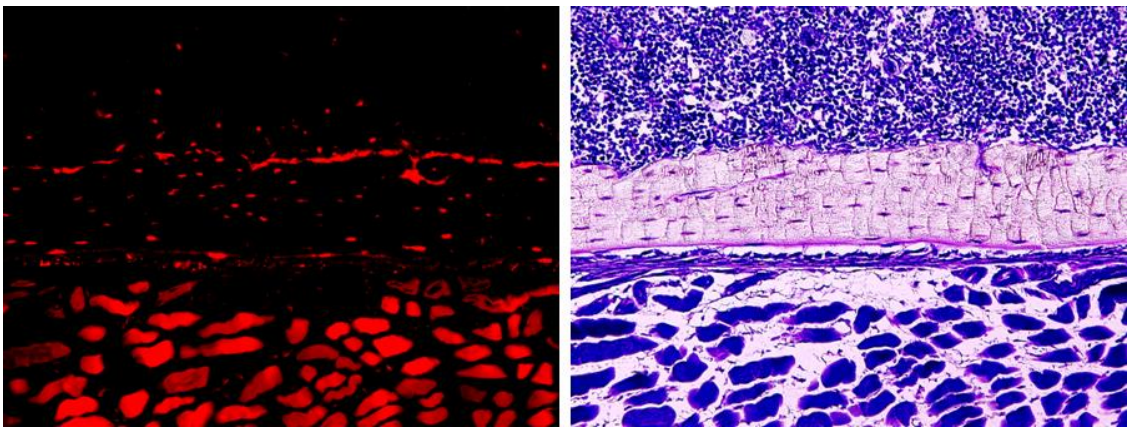

Figure 22C: Microscopic images of bone tissue from a *DMP1-Cre* positive mouse (without DAPI). Fluorescent (left) and toluidine blue stained (right) images of a bone tissue with muscle and marrow from a *DMP1-Cre* positive mouse. The fluorescent image shows red fluorescence in the muscle cells, osteoblasts and osteocytes. The marrow shows a few Cre positive red cells. The toluidine blue stained image shows the marrow, bone cells and muscle in purple color

Fluorescence White light (toluidine)

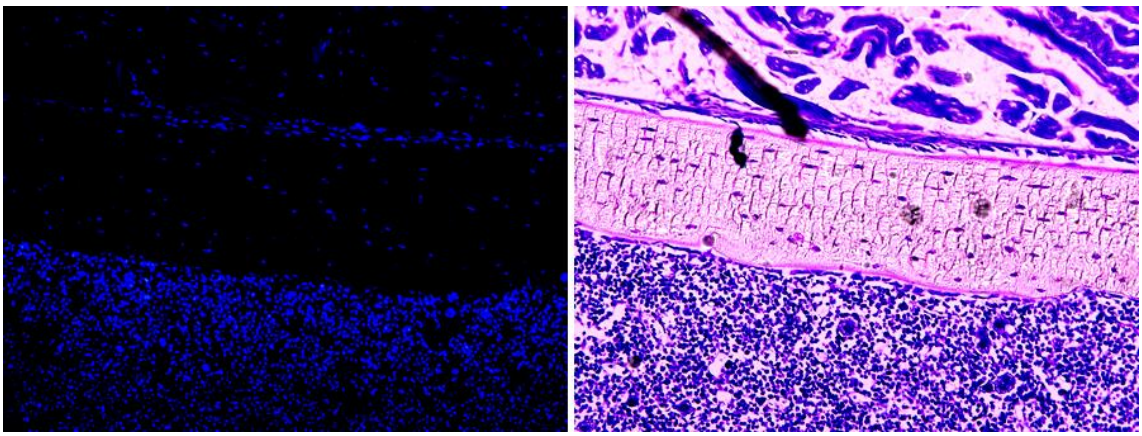

Figure 23: Microscopic images of bone tissue from a *DMP1-Cre* negative mouse. Fluorescent (left) and toluidine blue stained (right) images of a bone tissue with muscle and marrow from a *DMP1-Cre* negative mouse. In the fluorescent image the cell nuclei show blue color with DAPI staining. The toluidine blue stained image shows the marrow, bone cells and muscle in purple color.

3.7. Fluorescent microscopic and qualitative analysis results of the soft tissues from the *DMP1-Cre* mice:

To determine if there is nonspecific Cre-mediated recombination in the soft tissues of *DMP1-Cre* mouse line, the *Ai9* mice were crossed to the *DMP1-Cre* mice. The double positive (*Ai9+/DMP1-Cre+*) offspring were perfused and 5 um thick sections of different soft tissue such as heart, liver, kidney, spleen, duodenum and brain were prepared for histological analysis. The tissue sections were stained with DAPI. Figures 24 and 25 show fluorescent microscopic images (left) and toluidine blue stained white light images (right) of heart tissue from a *DMP1-Cre* positive and negative mouse respectively. Likewise, images 26-35 show the microscopic images of different tissues such as liver, kidney, duodenum, brain and spleen from the *DMP1-Cre* positive and negative mice. The result shows that there is no red fluorescence in the brain, and spleen tissue of *DMP1-Cre* positive mice. A few cells in heart, kidney, duodenum and liver show red fluorescent cells. The *DMP1-Cre* negative mice show no red fluoresce expression in any of the tested tissues.

Fluorescence white light (toluidine blue)

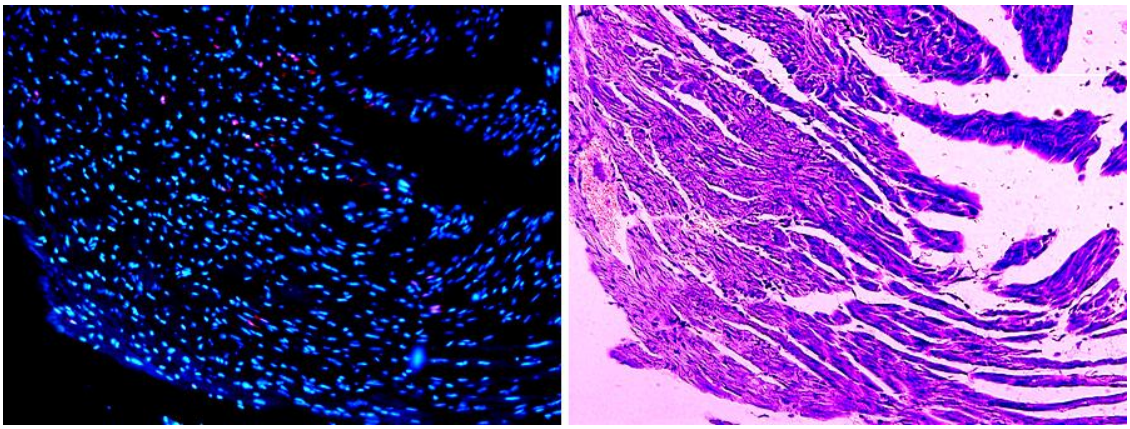

Figure 24: Microscopic images of heart tissue from a *DMP1-Cre* positive mouse
Fluorescent (left) and toluidine blue stained (right) images of heart tissue from a *DMP1-Cre* positive mouse. In the fluorescent image the DAPI stained nuclei appear as blue and a few cells shows red positive. The cells show purple color in the toluidine blue stained image.

Fluorescence white light (toluidine blue)

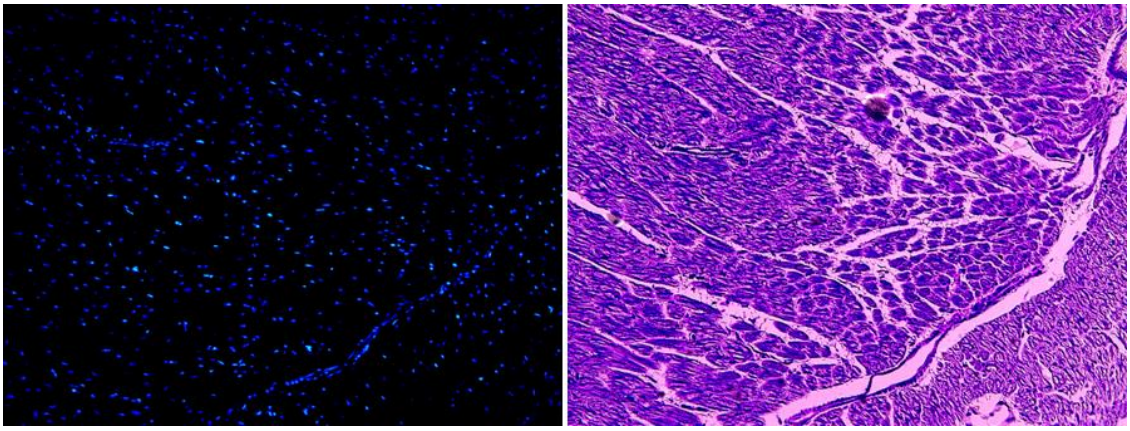

Figure 25: Microscopic images of heart tissue from a *DMP1-Cre* negative mouse.
Fluorescent (left) and toluidine blue stained (right) images of heart tissue from a *DMP1-Cre* negative mouse. In the fluorescent image, the nuclei appears as blue with DAPI staining. Cells show purple color in the toluidine blue stained image

Fluorescence White light (toluidine blue)

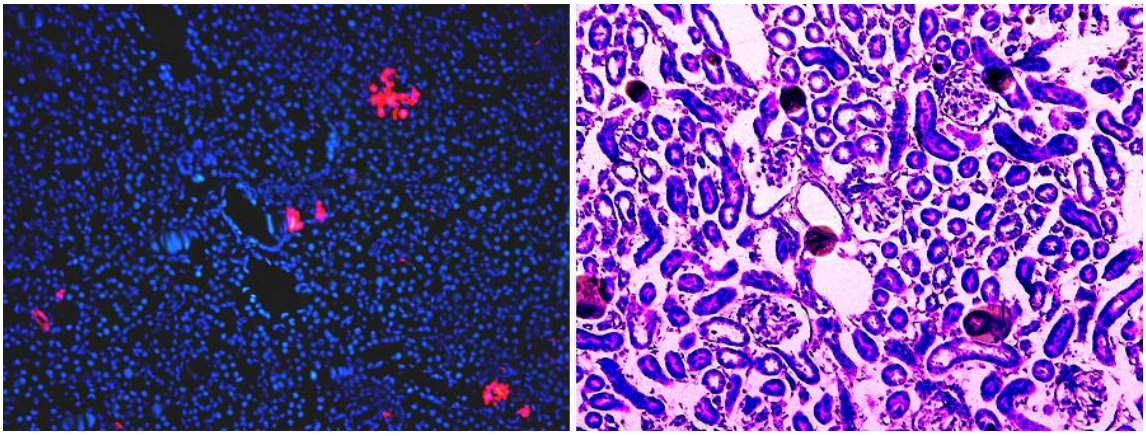

Figure 26: Microscopic images of kidney tissue from a *DMP1-Cre* positive mouse
Fluorescent (left) and toluidine blue stained (right) images of kidney tissue from a *DMP1-Cre* positive mouse. In the fluorescent image, the nuclei appears as blue with DAPI staining and a few cells show red positive. The cells appear in purple color in the toluidine blue stained image.

Fluorescence White light (toluidine blue)

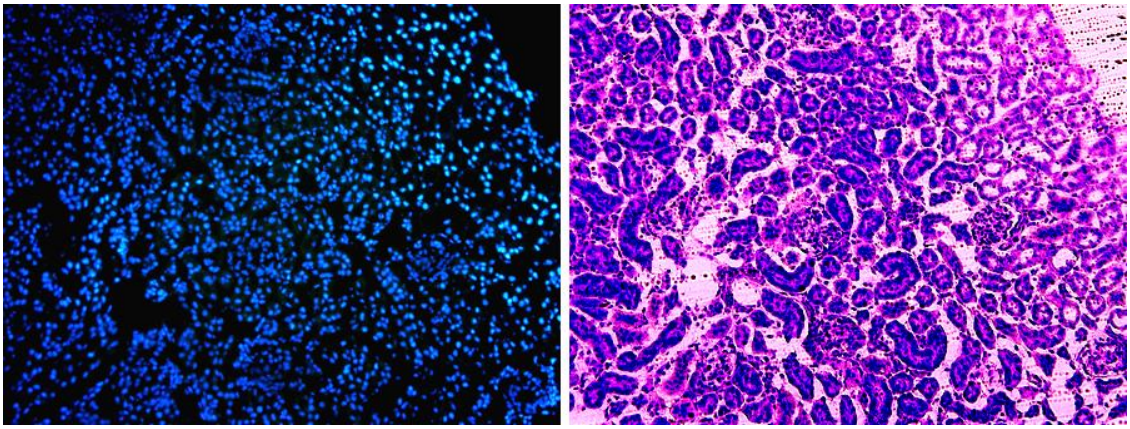

Figure 27: Microscopic images of kidney tissue from a *DMP1-Cre* negative mouse.
Fluorescent (left) and toluidine blue stained (right) images of kidney tissue from a *DMP1-Cre* negative mouse. In the fluorescent image, the nuclei appear as blue with DAPI staining. The cells appear in purple color in the toluidine blue stained image.

Fluorescence White light (toluidine blue)

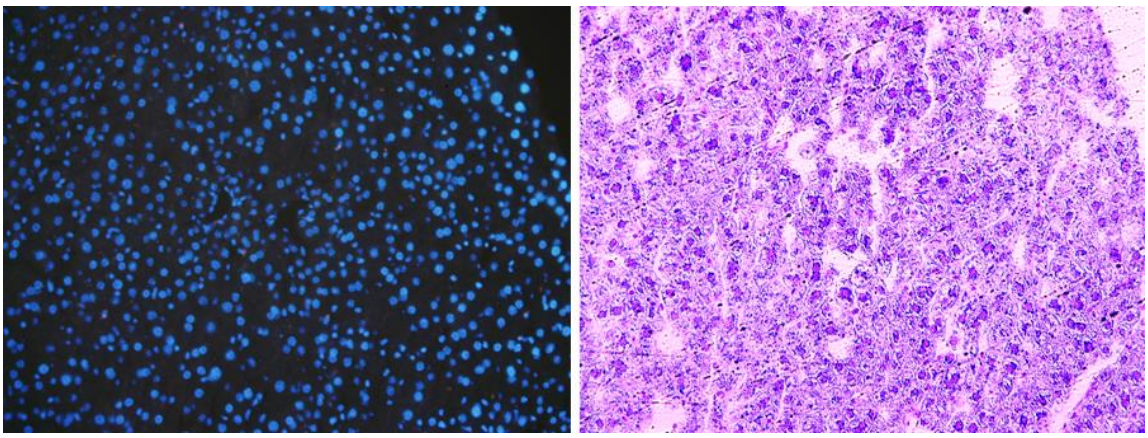

Figure 28: Microscopic images of liver tissue from a *DMP1-Cre* positive mouse. Fluorescent (left) and toluidine blue stained (right) images of liver tissue from a *DMP1-Cre* positive mouse. In the fluorescent image, the nuclei appear as blue with DAPI staining. The cells appear in purple color in the toluidine blue stained image.

Fluorescence White light (toluidine blue)

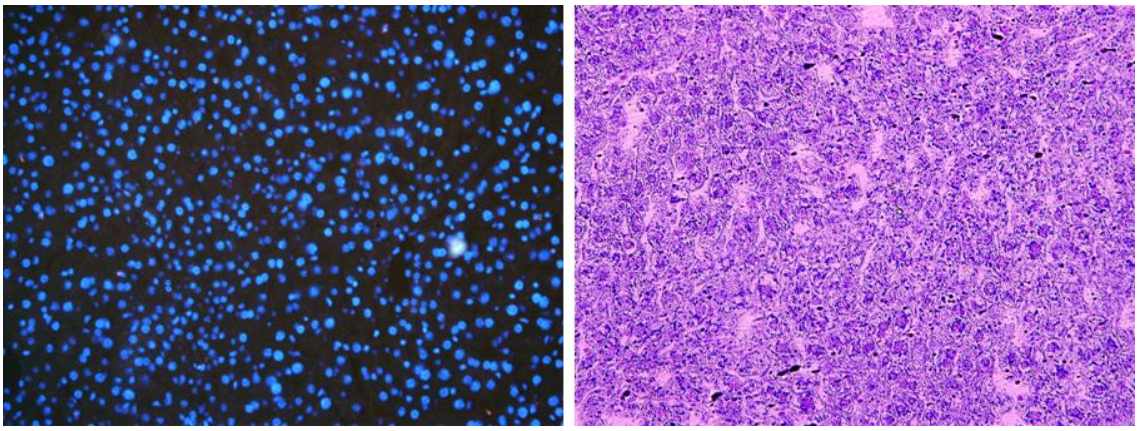

Figure 29: Microscopic images of liver tissue from a *DMP1-Cre* negative mouse. Fluorescent (left) and toluidine blue stained (right) images of liver tissue from *DMP1-Cre* negative mouse. In the fluorescent image, the nuclei appear as blue with DAPI staining. The cells appear in purple color in the toluidine blue stained image.

Fluorescence White light (toluidine blue)

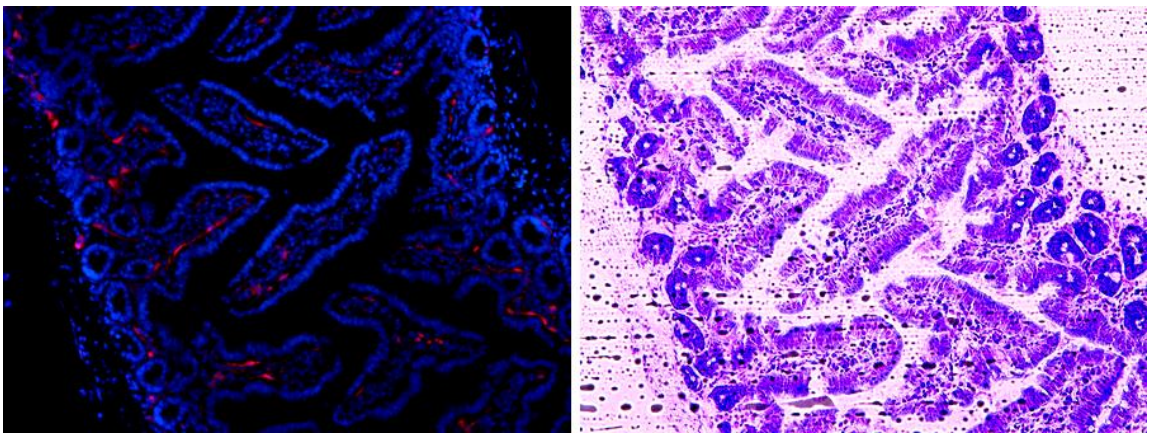

Figure 30: Microscopic images of duodenum tissue from a *DMP1-Cre* positive mouse. Fluorescent (left) and toluidine blue stained (right) images of duodenum tissue from a *DMP1-Cre* positive mouse. In the fluorescent image, the nuclei appear as blue with DAPI staining and a few cells show red positive. The cells appear in purple color in the toluidine blue stained image.

Fluorescence White light (toluidine blue)

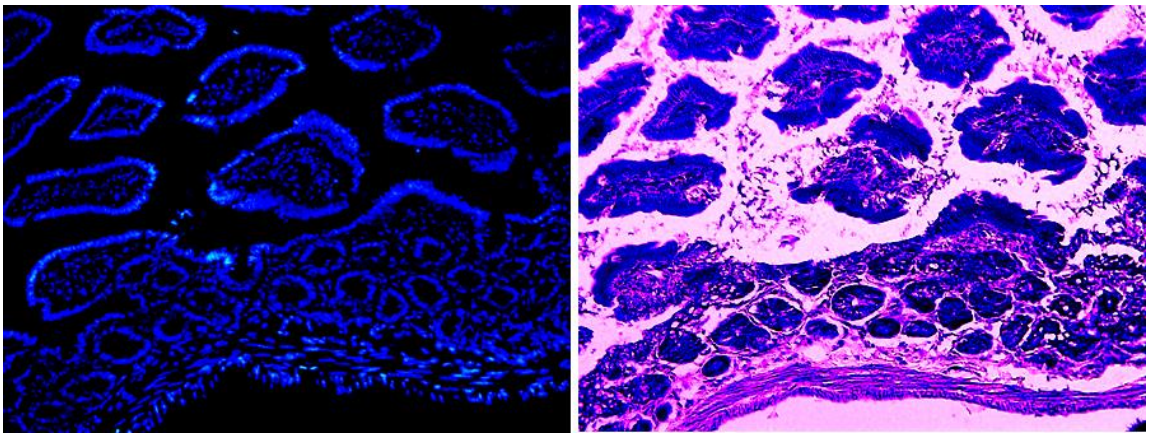

Figure 31: Microscopic images of duodenum tissue from a *DMP1-Cre* negative mouse. Fluorescent (left) and toluidine blue stained (right) images of duodenum tissue from a *DMP1-Cre* negative mouse. In the fluorescent image, the nuclei appear as blue with DAPI staining. The cells appear in purple color in the toluidine blue stained image.

Fluorescence White light (toluidine blue)

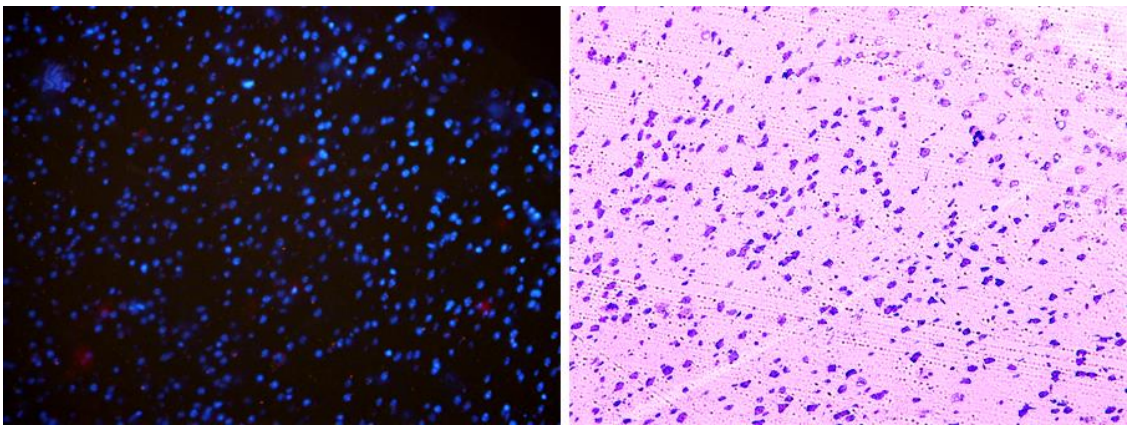

Figure 32: Microscopic images of brain tissue from a *DMP1-Cre* positive mouse. Fluorescent (left) and toluidine blue stained (right) images of brain tissue from a *DMP1-Cre* positive mouse. In the fluorescent image the nuclei appear as blue with DAPI staining. The cells appear in purple color in the toluidine blue stained image

Fluorescence White light (toluidine blue)

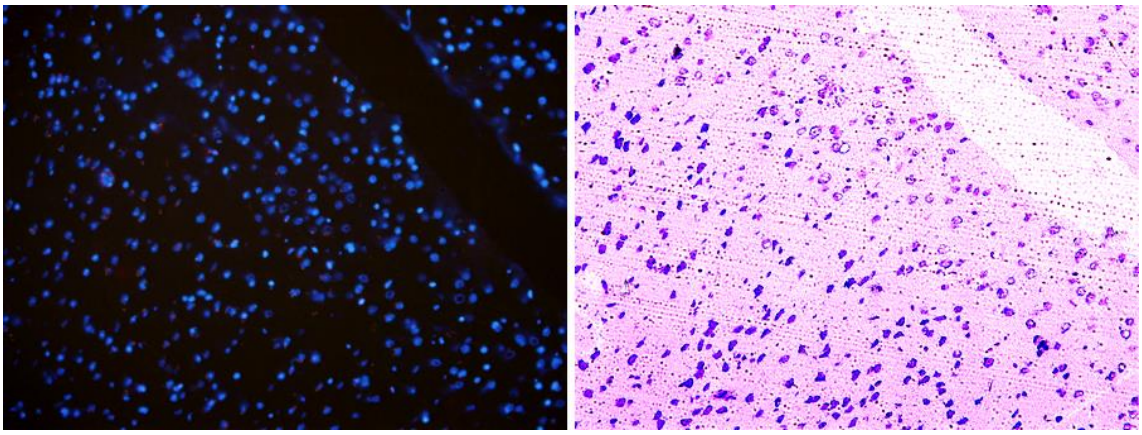

Figure 33: Microscopic images of brain tissue from a *DMP1-Cre* negative mouse. Fluorescent (left) and toluidine blue stained (right) images of brain tissue from a *DMP1-Cre* negative mouse. In the fluorescent image, the nuclei appear as blue with DAPI staining. The cells appear in purple color in the toluidine blue stained image**.**

Fluorescence White light (toluidine blue)

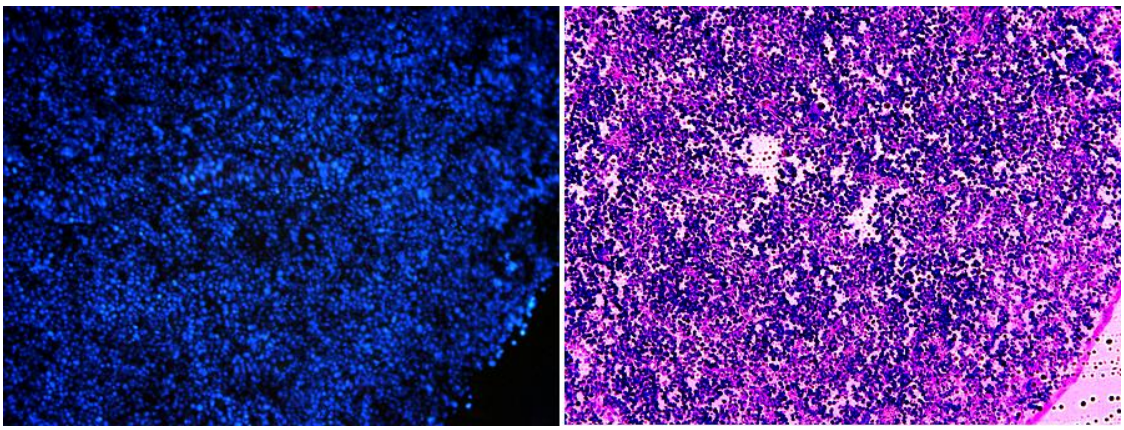

Figure 34: Microscopic images of spleen tissue from a *DMP1-Cre* positive mouse. Fluorescent (left) and toluidine blue stained (right) images of spleen tissue from a *DMP1-Cre* positive mouse. In the fluorescent image the nuclei appear as blue with DAPI staining. The cells appear in purple color in the toluidine blue stained image.

Fluorescence White light (toluidine blue)

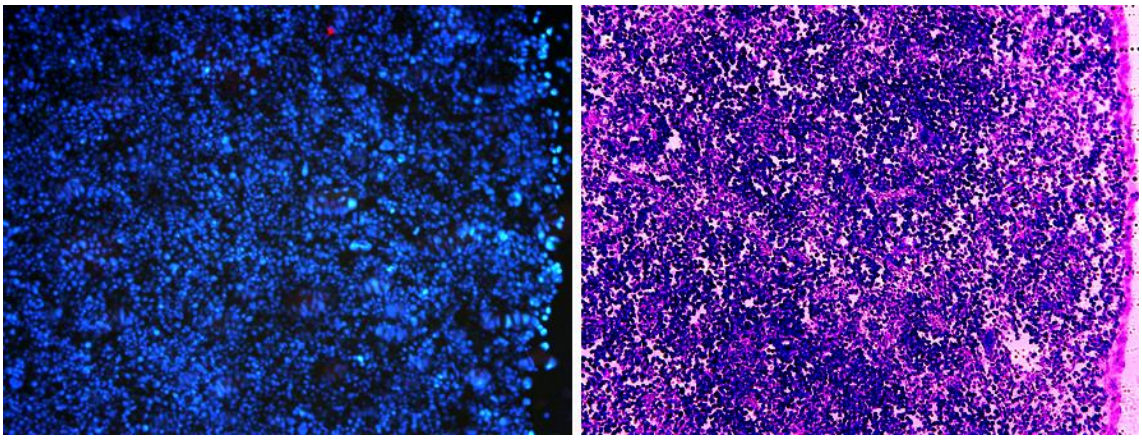

Figure 35: Microscopic images of spleen tissue from a *DMP1-Cre* negative mouse. Fluorescent (left) and toluidine blue stained (right) images of spleen tissue from a *DMP1-Cre* negative mouse. In the fluorescent image, the nuclei appear as blue with DAPI staining. The cells appear in purple color in the toluidine blue stained image.

3.8. Results of quantitation of positive Cre-expressing cells in the bone and soft tissues of the *DMP1-Cre* mice by ImageJ cell counting:

To study the effect of Cre-mediated recombination in the tissues of *DMP1-Cre* mouse line, fluorescence microscopic analysis of 5um thick sections of the femur bone and soft tissues from the double positive (*Ai9+/DMP1-Cre+)* mice was performed. The tissue sections were analyzed for positive red color fluorescence which is an indication of Cre-recombinase. Fluorescence positive cells were quantitated using ImageJ software program. The total number of cells were counted using ImageJ automated counting tool and the red positive cells in each positive Cre-expressing tissue samples were counted manually. The result of the cell quantitation from the positive Cre-expressing tissue are listed in Table 2.

The average of percentage of the Cre-expression from the studied three mice and their standard deviations are listed in Table 3.

Figure 36 is a Bar chart showing Cre recombinase expression in the bone and all tested soft tissues from the three *DMP1-Cre* mice used in this study.

DMP-Cre											
		Bone marrow		**Osteocytes**		**Heart**		**Kidney**		**Duodenum**	
		Total number of cells	Number of positive cells	Total number of cells	Number of positive cells	Total number of cells	Number of positive cells	Total number of cells	Number of positive cells	Total number of cells	Number of positive cells
Mouse 1	Sample1	3082	12	61	41	1101	1	2710	0	1775	87
	Sample2	7034	4	83	72	1064	0	2405	17	1035	16
	Sample3	2965	34	51	43	1036	0	2330	0	2154	173
Mouse 2	Sample1	2977	41	87	79	1252	0	2859	17	1733	61
	Sample2	3944	47	98	87	1583	7	2115	22	1609	112
	Sample3	2709	12	129	104	1528	4	2611	4	1114	56
Mouse 3	Sample1	3288	5	62	55	897	2	2607	10	2859	61
	Sample2	3609	0	43	36	1218	13	2049	10	2115	62
	Sample3	4369	1	55	50	1243	10	8328	0	2611	40

Table 2: Cell quantitation result from the different tissues of the three *DMP1-Cre* mice used in this study.

% of Cre exprssion in *DMP1-Cre* mice tissues[(number of positive cell/Total number of cells) X 100]									
		Bone marrow	**Osteocytes**	**heart**	**kidney**	**liver**	**brain**	**Duodenum**	**Spleen**
Mouse 1	sample								
	1	0.4	83.6	0.09	0	0.18	0	4.9	0
	2	0.01	86.8	0	0.71	0	0	1.55	0
	3	1.15	84.3	0	0	0.075	0	8.03	0
Average		0.52	84.9	0.03	0.23667	0.085	0	4.8266667	0
Standard deviation		0.579396237	1.68226038	0.05196	0.40992	0.09042	0	3.2406224	0
Mouse 2	sample								
	1	1.38	90.8	0	0.59	0	0	3.52	0
	2	1.19	88.8	0.44	1.04	0	0	6.95	0
	3	0.44	80.6	0.26	0.15	0.43	0	5.03	0
Average		1.003333333	86.7333333	0.23333	0.59333	0.14333	0	5.1666667	0
Standard deviation		0.49702448	5.40493602	0.22121	0.44501	0.24826	0	1.7190792	0
Mouse 3	Sample								
	1	0.15	88.8	0.22	0.38	0	0	0.03	0
	2	0	83.7	1.08	0.49	0	0	0.3	0
	3	2.3	90.9	0.8	0	0	0	0.1	0
Average			87.8	0.7	0.29	0	0	0.1433333	0
Standard deviation		1.286791876	3.70270172	0.43863	0.2571	0	0	0.140119	0

Table 3: Result of quantitation of positive Cre-expression and its standard deviation from the different tissues of the three *DMP1-Cre* mice used in this study.

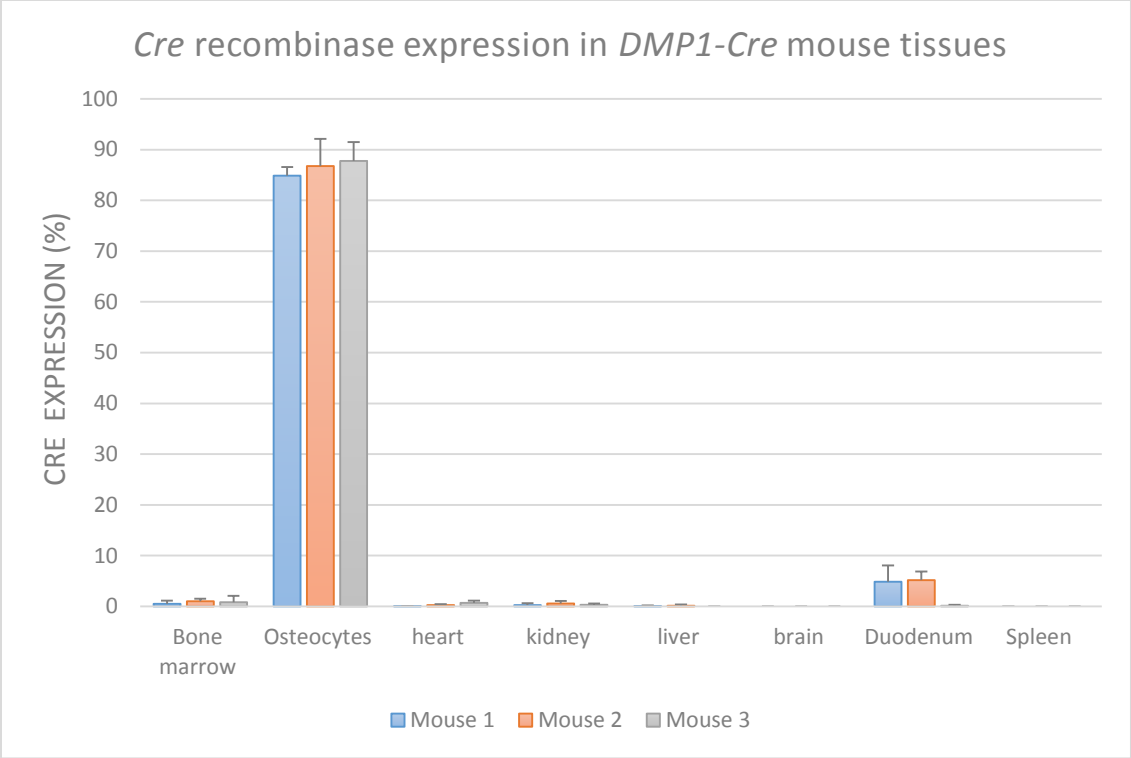

Figure 36: Bar chart showing percentage of Cre recombinase expression from the different tissues of the three *DMP1-Cre* mice used in this study.

3.9. PCR results indicating the presence of *Ctsk-Cre* transgene:

PCR was performed with ear tissue samples from the offspring of the breeders - *Ctsk-Cre* female and Ai9 male to detect the presence of *Ctsk-Cre* transgene, using the respective primers. The gel was analyzed for the presence of 600 bp band of *Ctsk-Cre* transgene and 1000bp band of *connexin-43* internal control. Figure 37 shows PCR followed by agarose gel electrophoresis from *Ctsk-Cre* mice tissue.

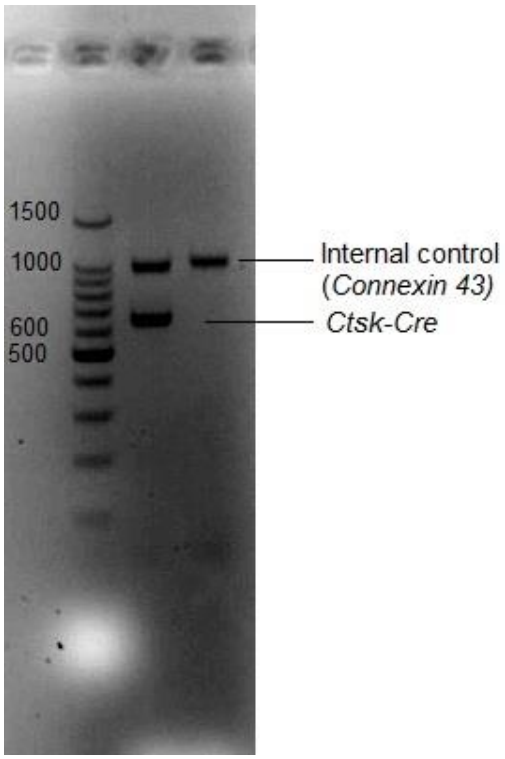

Figure 37: Agarose gel showing *Ctsk-Cre* band. The first lane shows the DNA ladder. The second lane is a positive sample which shows 2 bands. The high band is internal control *Connexin-43* that aligns with 1000bp band of the ladder and the low 600bp band is *Ctsk-Cre*. The third lane shows a negative sample which shows only the internal control *Connexin-43.*

3.10. Fluorescence microscopic and qualitative analysis results of the bone tissues from the *Ctsk-Cre* mice:

To determine if there is Cre-mediated recombination in the bone tissue of *Ctsk-Cre* mouse line, the Ai9 mice was crossed to the *Ctsk-Cre* mice. The double positive (*Ai9+/Ctsk-Cre+*) offspring were perfused and 5 um thick sections of the femur bone tissue were prepared for histological analysis. The bone tissue sections were stained with DAPI. Figures 38a and 39a show fluorescent microscopic images (left) and toluidine blue stained white light images (right) of bone tissue from a *Ctsk-Cre* positive mouse. Red fluorescent osteoclasts residing on the bone surface, appearing with ruffled borders, can be seen. Some of the osteocytes in the bone matrix, and a few cells in the marrow also show red fluorescence which can be quantitated. There is no Cre-expression in muscle tissue. Figures 38b and 39b show bone tissue from a *Ctsk-Cre* mouse without DAPI nuclear stain, which also yielded strong positive fluorescence in osteoclasts. Figures 40 and 41 of the bone marrow show red fluorescence in a few cells residing on bone surface, which indicates Cre-expression in osteoclasts (Cathepsin K). Figure 42 (reproduced from Reference 27) shows H&E stained bone tissue. The brown color on the surface indicates Cathepsin K localization in osteoclasts. Figure 43 shows newly forming bone with osteoblasts and osteocytes which shows no red fluorescence, supporting the lack of Cre-expression in osteoblasts and osteocytes. Figure 44 shows bone tissue from a *Ctsk-Cre* negative control mouse which yielded no red fluorescence in bone, marrow and muscle cells. The microscopic qualitative analysis of bone tissue

from *Ctsk-Cre* positive mice show that there is significant Cre-expression in osteoclasts. There are a few red positive cells in marrow and osteocytes.

Fluorescence White light (toluidine blue)

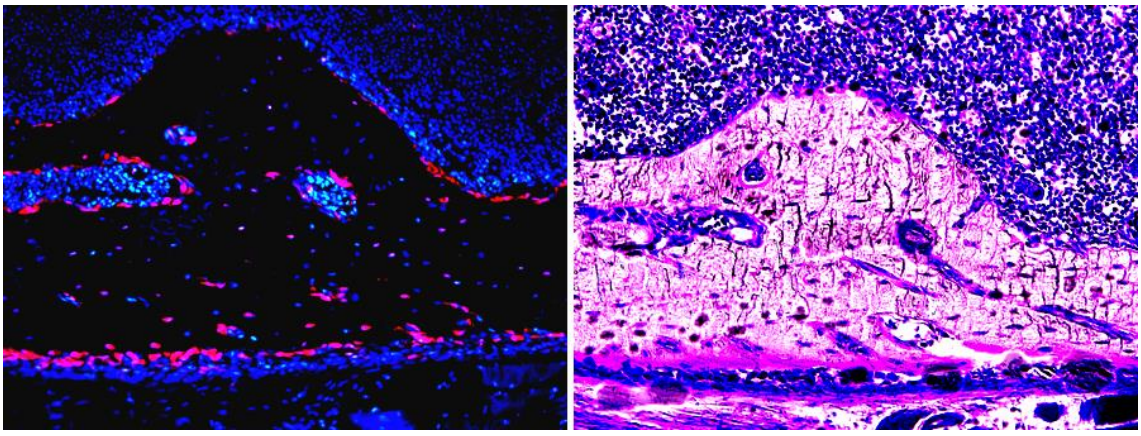

Figure 38a: Microscopic images of bone tissue with marrow and muscle from a *Ctsk-Cre* positive mouse (DAPI stained). Fluorescent (left) and toluidine blue stained (right) images of bone tissue with muscle and marrow from a *Ctsk-Cre* positive mouse. The fluorescent image shows red fluorescence in osteoclasts located on the bone surface. A few osteocytes on in the matrix show positive expression. The marrow shows blue color with DAPI nuclear staining. The toluidine blue stained image shows the marrow, bone matrix and muscle in purple color.

Fluorescence White light (toluidine blue)

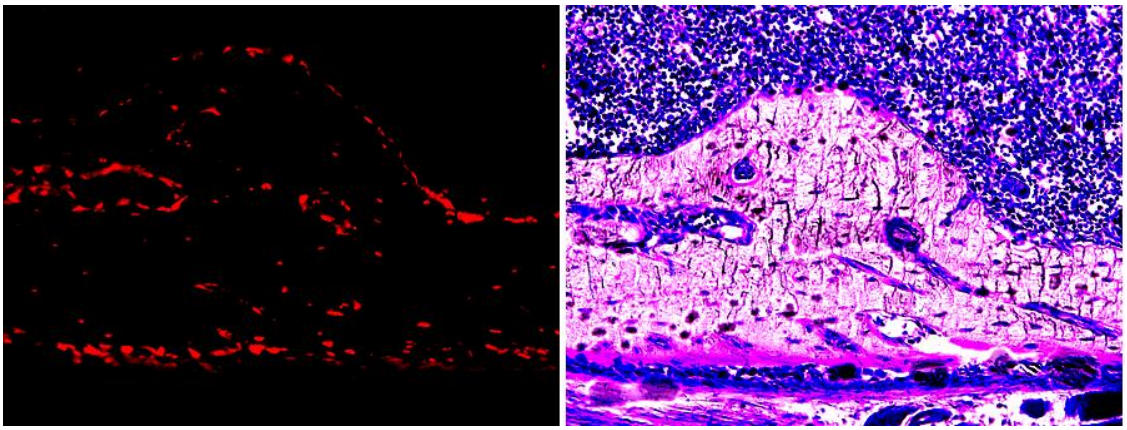

Figure 38b: Microscopic images of bone tissue with marrow and muscle from a *Ctsk-Cre* positive mouse (without DAPI). Fluorescent (left) and toluidine blue stained (right) images of bone tissue with muscle and marrow from a *Ctsk-Cre* positive mouse. The fluorescent image shows red fluorescence in osteoclasts located on the bone surface. A few osteocytes on the matrix show positive red.The toluidine blue stained image shows the marrow, bone matrix and muscle in purple color.

Fluorescence White light (toluidine blue)

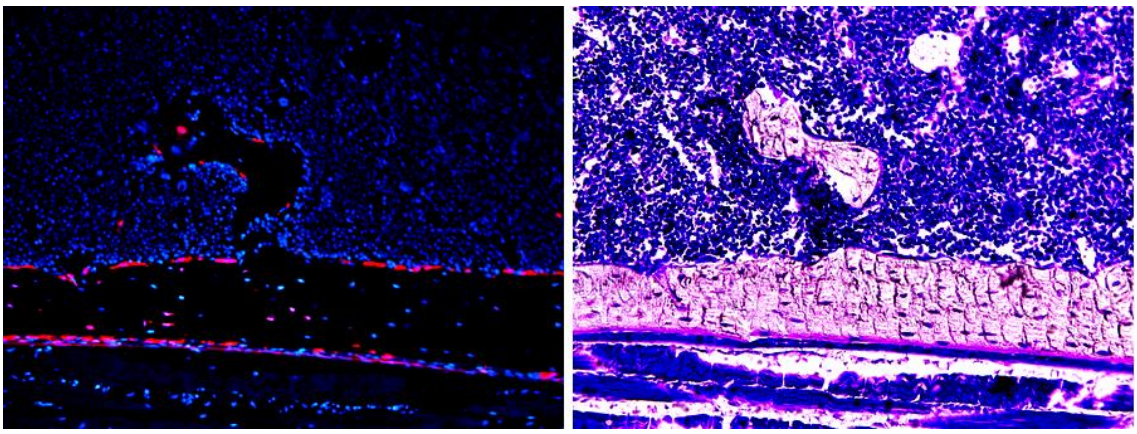

Figure 39a: Microscopic images of bone tissue with marrow and muscle from a *Ctsk-Cre* positive mouse (DAPI stained). Fluorescent (left) and toluidine blue stained (right) images of bone tissue with muscle and marrow from a *Ctsk-Cre* positive mouse. The fluorescent image shows red fluorescence in osteoclasts located on the bone surface. A few osteocytes in the matrix show red positive. The marrow shows blue color with DAPI nuclear staining. The toluidine blue stained image shows the marrow, bone matrix and muscle in purple color.

Fluorescence White light (toluidine blue)

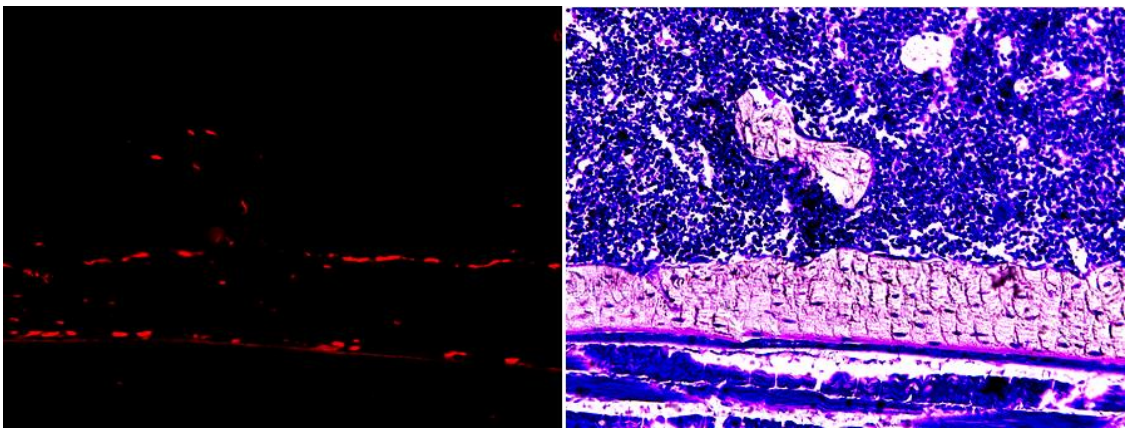

Figure 39b: Microscopic images of bone tissue with marrow and muscle from a *Ctsk-Cre* positive mouse (without DAPI). Fluorescent (left) and toluidine blue stained (right) images of bone tissue with muscle and marrow from a *Ctsk-Cre* positive mouse. The fluorescent image shows red fluorescence in osteoclasts located on the bone surface. The marrow shows blue color with DAPI nuclear staining. The toluidine blue stained image shows the marrow, bone matrix and muscle in purple color.

Fluorescence White light (toluidine blue)

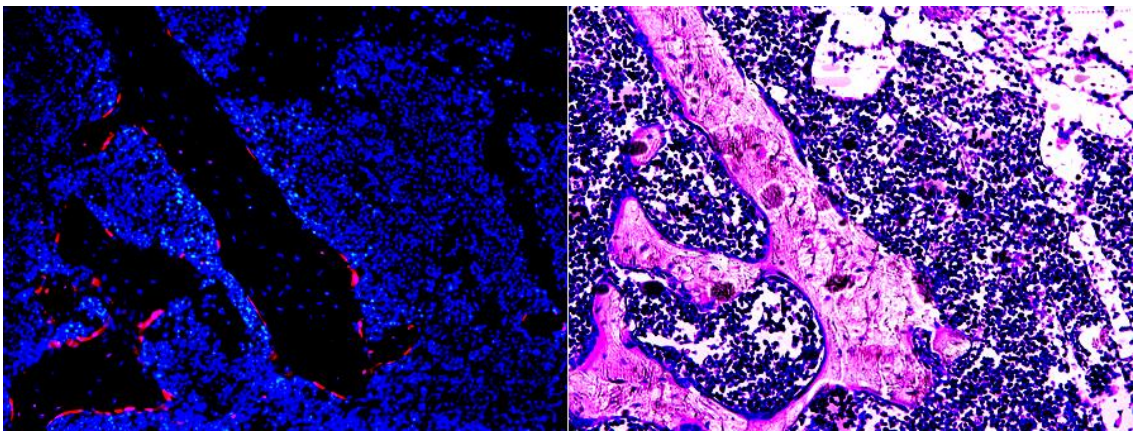

Figure 40a: Microscopic images of bone tissue with marrow and muscle from a *Ctsk-Cre* positive mouse (DAPI stained). Fluorescent (left) and toluidine blue stained (right) images of bone tissue with marrow from a *Ctsk-Cre* positive mouse. The fluorescent image shows red fluorescence in osteoclasts located on the bone surface. The marrow shows blue color with DAPI nuclear staining. The toluidine blue stained image shows the marrow, bone matrix and muscle in purple color.

Fluorescence White light (toluidine blue)

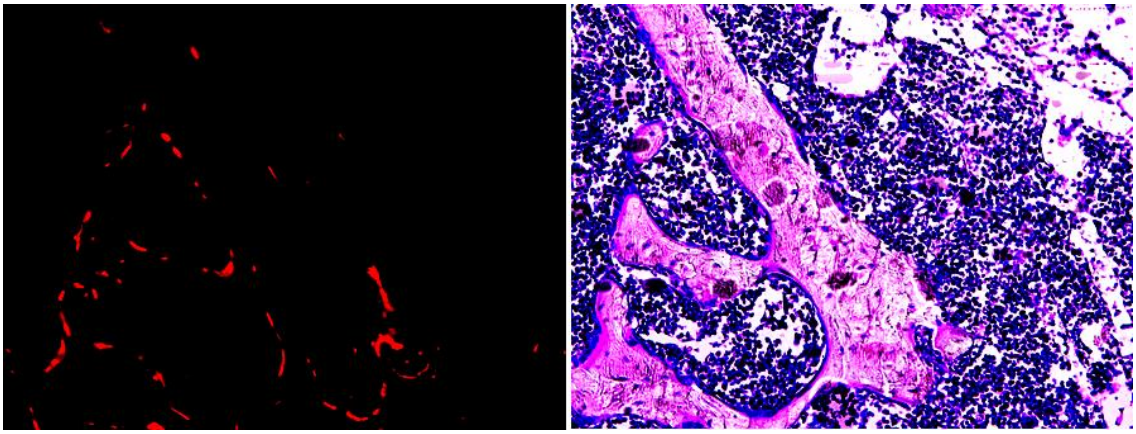

Figure 40b: Microscopic images of bone tissue with marrow and muscle from a *Ctsk-Cre* positive mouse (without DAPI). Fluorescent (left) and toluidine blue stained (right) images of bone tissue with marrow from a *Ctsk-Cre* positive mouse. The fluorescent image shows red fluorescence in osteoclasts located on the bone surface. The toluidine blue stained image shows the marrow, bone matrix and muscle in purple color.

Fluorescence White light (toluidine blue)

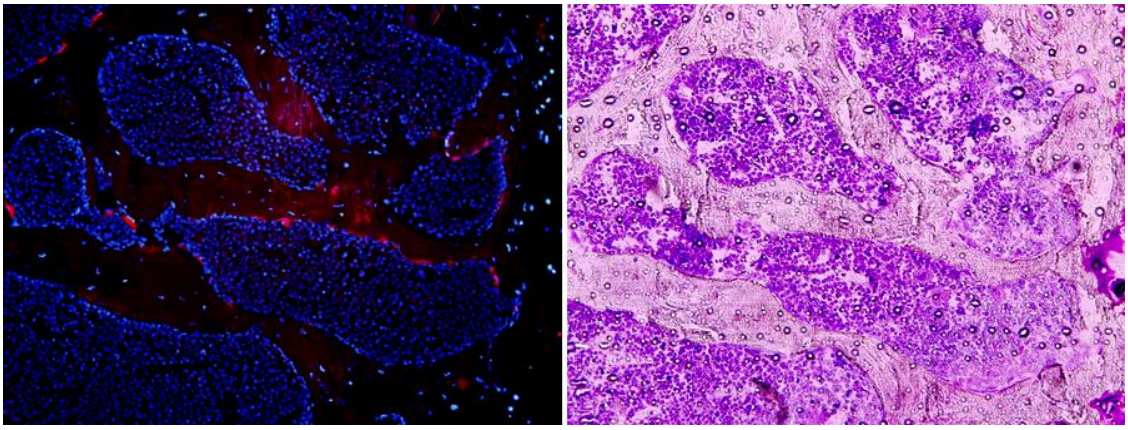

Figure 41: Microscopic images of bone tissue with marrow from a *Ctsk-Cre* positive mouse. Fluorescent (left) and toluidine blue stained (right) images of bone tissue with marrow from a *Ctsk-Cre* positive mouse. The red color dots on the surface indicate the presence of osteoclasts. The marrow shows blue color with DAPI nuclear staining. The toluidine blue stained image shows the marrow, bone matrix and muscle in purple color.

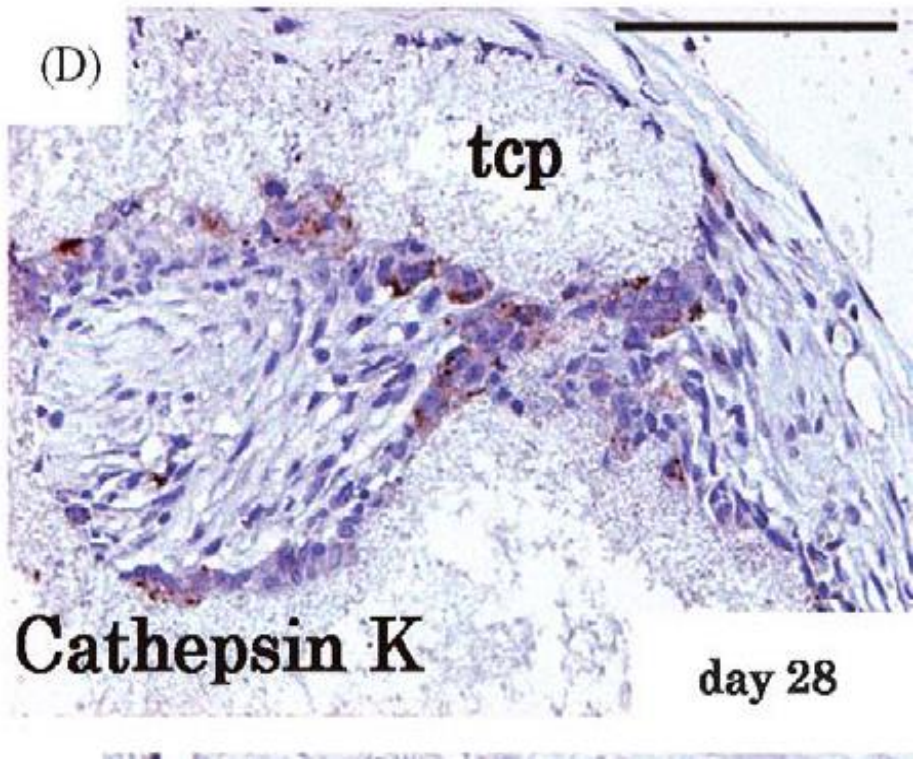

Figure 42: Cathepsin K localization in osteoclast (reference 27). H&E stained bone tissue. The brown color on the bone surface indicates Cathepsin K localized in osteoclasts.

Fluorescence White light (toluidine blue)

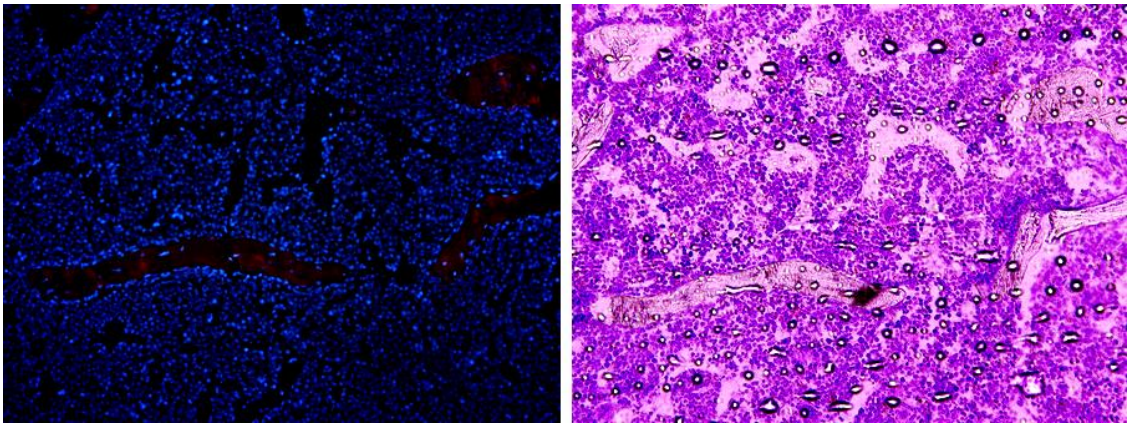

Figure 43: Microscopic images of bone tissue from a *Ctsk-Cre* positive mouse (osteoblasts and osteocytes). Bone marrow with newly forming bone tissue from a *Ctsk-Cre* positive mouse. Absence of red color in the fluorescent image supports that there is no Cre-expression in osteoblast or osteocytes. The marrow appears as blue with DAPI nuclear staining. The toluidine blue stained image shows marrow in purple color.

Fluorescence White light (toluidine blue)

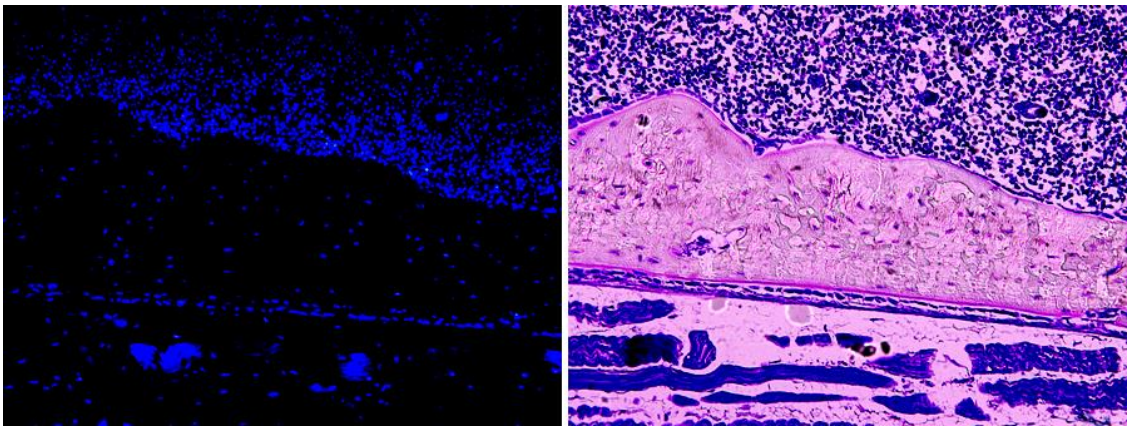

Figure 44: Microscopic images of bone tissue with marrow and muscle from a *Ctsk-Cre* negative mouse. Microscopic images of bone tissue with marrow and muscle from a *Ctsk-Cre* negative mouse Fluorescent (left) and toluidine blue stained (right) images of bone tissue with muscle and marrow from a *Ctsk-Cre* negative mouse. In the fluorescent image the cell nuclei give blue color with DAPI staining. The toluidine blue stained image shows the marrow, bone matrix and muscle in purple color.

3.11. Fluorescence microscopic and qualitative analysis results of the soft tissues from the *Ctsk-Cre* mice:

To determine if there is nonspecific Cre-mediated recombination in the soft tissues of *Ctsk-Cre* mouse line, the Ai9 mice were crossed to the *Ctsk-Cre* mice. The double positive (*Ai9+/Ctsk-Cre+*) offspring were perfused and 5 um thick sections of the tissue such as heart, kidney, liver, brain, duodenum and spleen were prepared for histological analysis. The tissue sections were stained with DAPI. Figures 45 and 46 show fluorescent microscopic images (left) and toluidine blue stained white light images (right) of heart tissue from a *Ctsk-Cre* positive and negative mouse respectively. Likewise, figures 47-55 show the microscopic images of different soft tissues such as liver, kidney, duodenum, brain and spleen from the *Ctsk-Cre* positive and negative mice. The result shows that there is no Cre-expression in duodenum and spleen cells of *Ctsk-Cre* positive mouse. A few cells in kidney, liver and heart tissues show red fluorescence. However, brain tissue yielded significant red fluorescence. All the tested soft tissues from negative control *Ctsk-Cre* mice show negative fluorescence.

Fluorescence White light (toluidine blue)

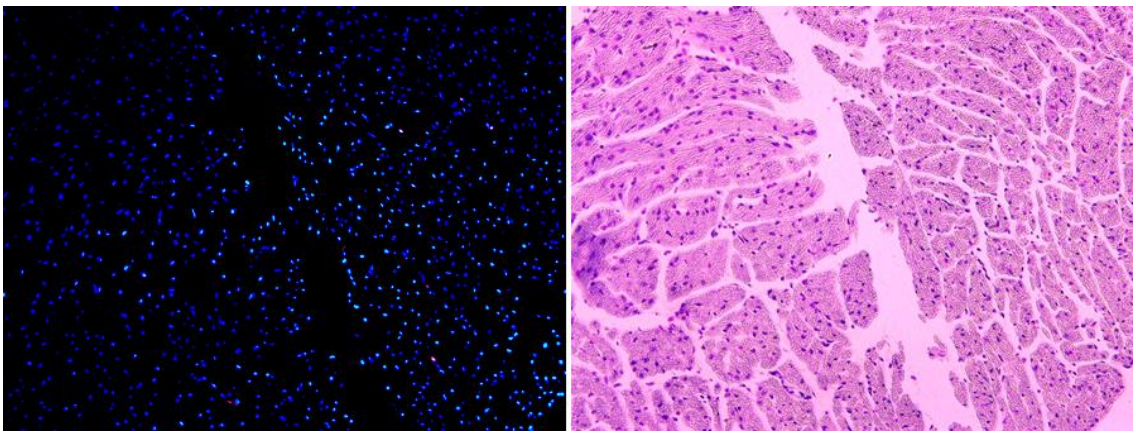

Figure 45: Microscopic images of heart tissue from a *Ctsk-Cre* positive mouse. Fluorescent (left) and toluidine blue stained (right) images of heart tissue from a *Ctsk-Cre* positive mouse. In the fluorescent image, the nuclei appear as blue with DAPI staining. The cells appear in purple color in the toluidine blue stained image.

Fluorescence White light (toluidine blue)

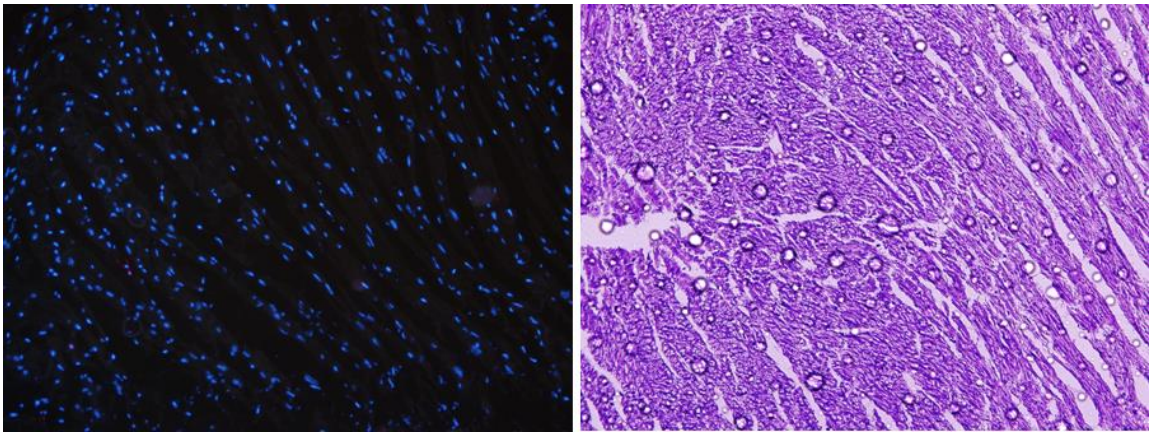

Figure 46: Microscopic images of heart tissue from a *Ctsk-Cre* negative mouse. Fluorescent (left) and toluidine blue stained (right) images of heart tissue from a *Ctsk-Cre* negative mouse. In the fluorescent image, the nuclei appears as blue with DAPI staining. The cells appear in purple color in the toluidine blue stained image.

Fluorescence White light (toluidine blue)

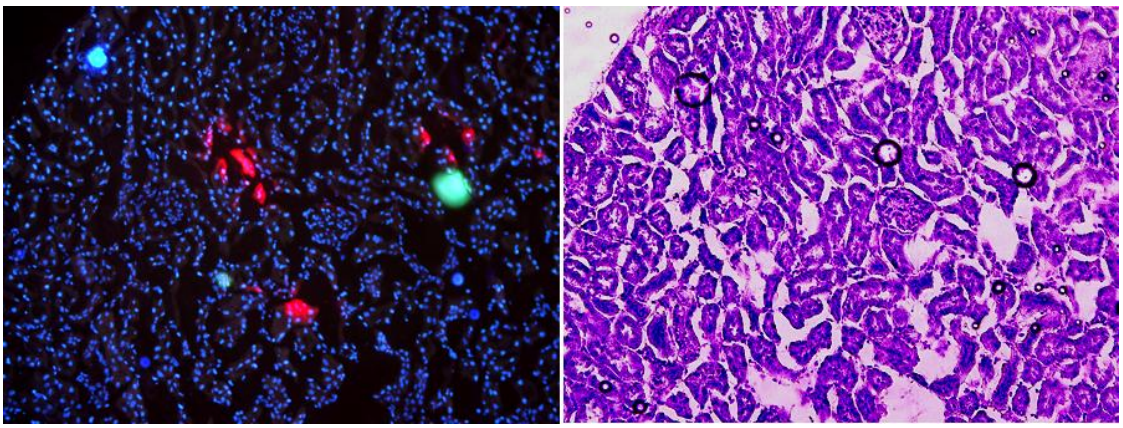

Figure 47: Microscopic images of kidney tissue from a *Ctsk-Cre* positive mouse. Fluorescent (left) and toluidine blue stained (right) images of kidney tissue from a *Ctsk-Cre* positive mouse. In the fluorescent image, the nuclei appear as blue with DAPI staining and a few cells shows red positive. The cells appear in purple color in the toluidine blue stained image.

Fluorescence White light (toluidine blue)

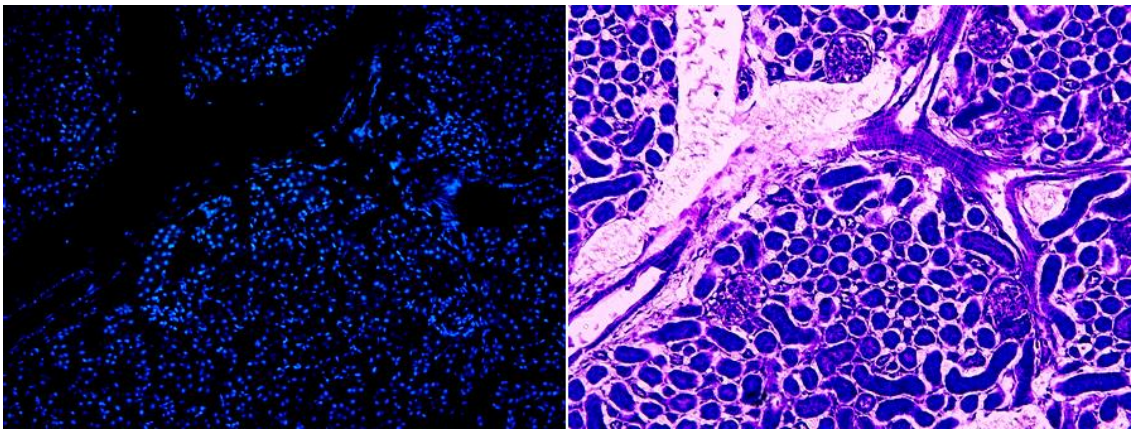

Figure 48: Microscopic images of kidney tissue from a *Ctsk-Cre* negative mouse. Fluorescent (left) and toluidine blue stained (right) images of kidney tissue from a *Ctsk-Cre* negative mouse. In the fluorescent image, nuclei appear as blue with DAPI staining. The cells appear in purple color in the toluidine blue stained image

Fluorescence White light (toluidine blue)

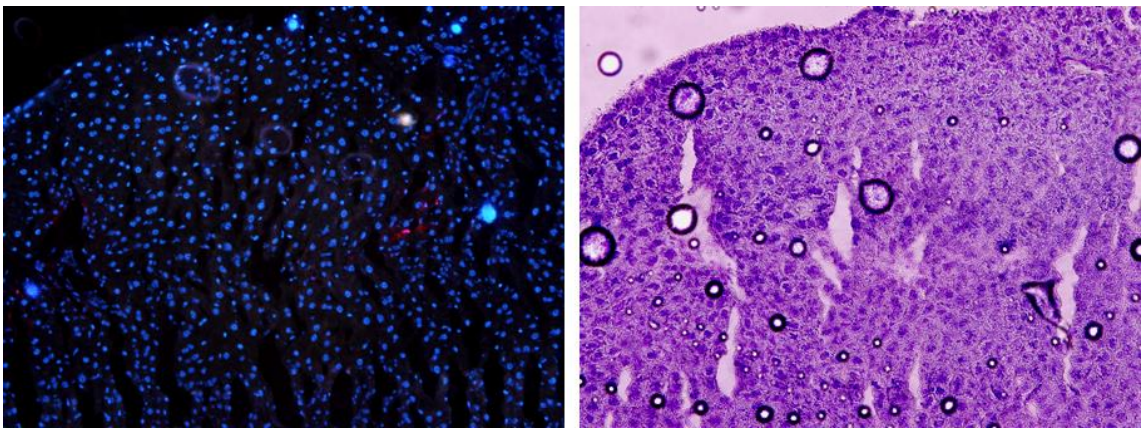

Figure 49: Microscopic images of liver tissue from a *Ctsk-Cre* positive mouse. Fluorescent (left) and toluidine blue stained (right) images of liver tissue from a *Ctsk-Cre* positive mouse. In the fluorescent image, the nuclei appears as blue with DAPI staining and a few cells shows red positive. The cells appear in purple color in the toluidine blue stained image

Fluorescence White light (toluidine blue)

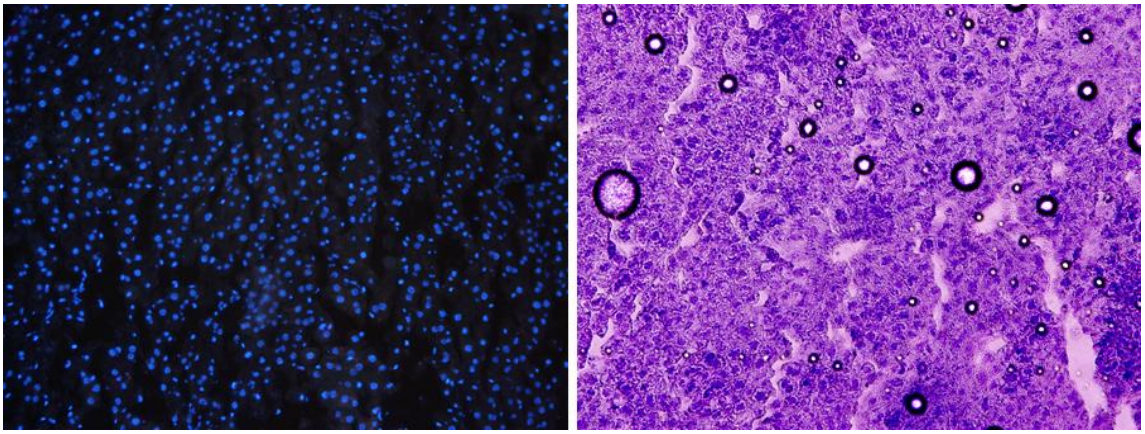

Figure 50: Microscopic images of liver tissue from a *Ctsk-Cre* negative mouse. Fluorescent (left) and toluidine blue stained (right) images of liver tissue from a *Ctsk- Cre* negative mouse. In the fluorescent image, the nuclei appears as blue with DAPI staining. The cells appear in purple color in the toluidine blue stained image.

Fluorescence White light (toluidine blue)

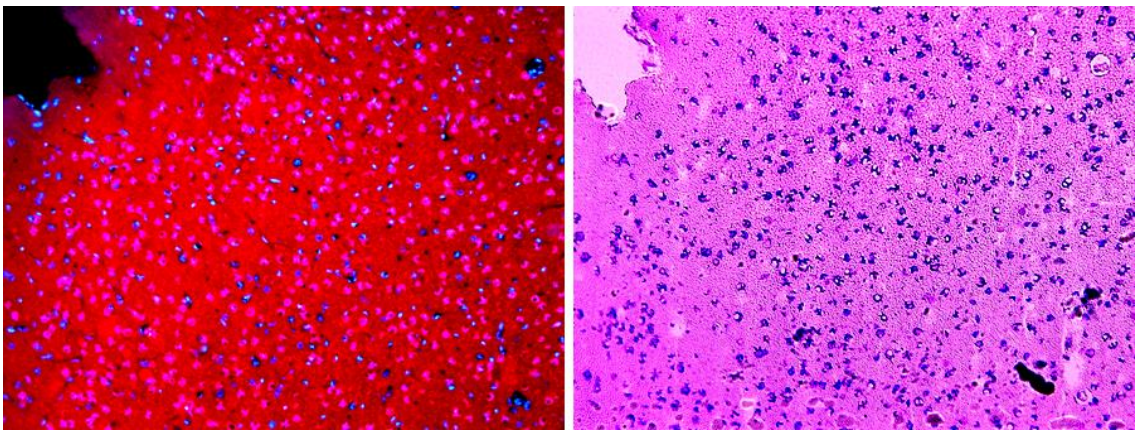

Figure 51a: Microscopic images of brain tissue from a *Ctsk-Cre* positive mouse. Fluorescent (left) and toluidine blue stained (right) images of brain tissues from a *Ctsk-Cre* positive mouse. The fluorescent images show bright red color since the entire cells have turned into red with positive Cre-expression. The nuclei appear as blue with DAPI staining. The cells appear in purple color in the toluidine blue stained image.

Fluorescence White light (toluidine blue)

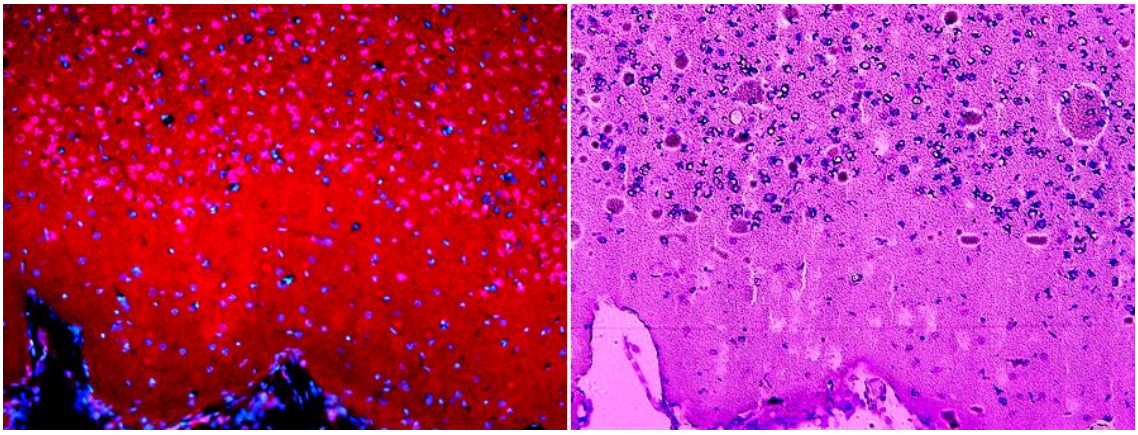

Figure 51b: Microscopic images of brain tissue from a *Ctsk-Cre* positive mouse. Fluorescent (left) and toluidine blue stained (right) images of brain tissues from a *Ctsk-Cre* positive mouse. The fluorescent images show bright red color since the entire cells have turned into red with positive Cre expression. The nuclei appear as blue with DAPI staining. The cells appear in purple color in the toluidine blue stained image.

Fluorescence White light (toluidine blue)

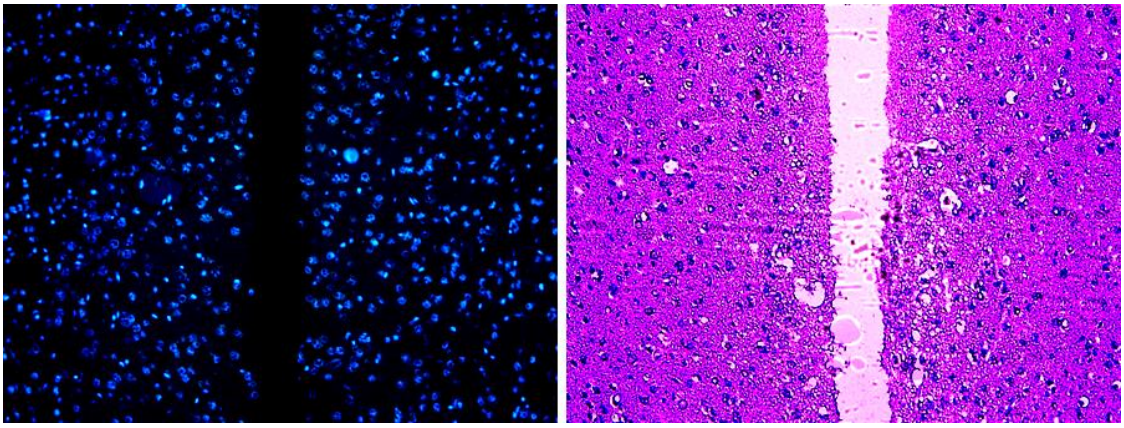

Figure 52: Microscopic images of brain tissue from a *Ctsk-Cre* negative mouse. Fluorescent (left) and toluidine blue stained (right) images of brain tissue from a *Ctsk-Cre* negative mouse. In the fluorescent image, the nuclei appear as blue with DAPI staining. The cells appear in purple color in the toluidine blue stained image.

Fluorescence White light (toluidine blue)

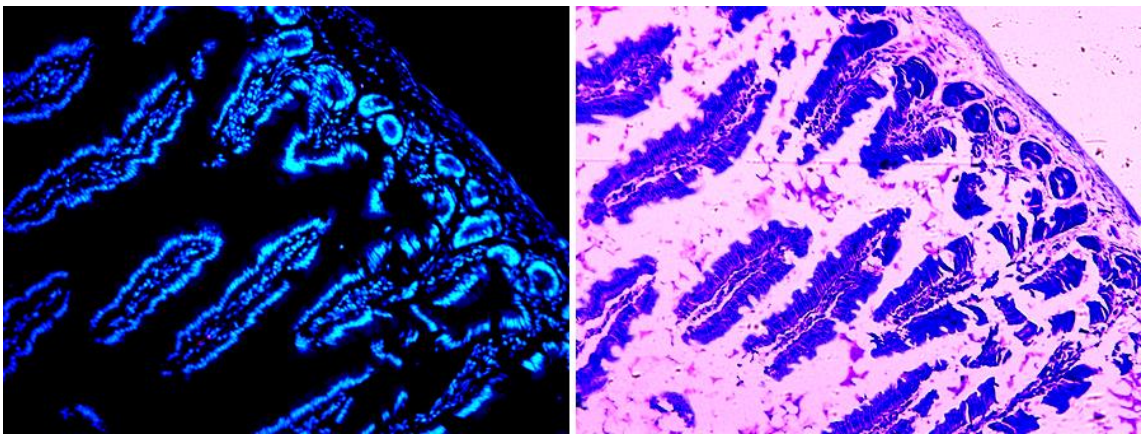

Figure 53: Microscopic images of duodenum tissue from a *Ctsk-Cre* positive mouse. Fluorescent (left) and toluidine blue stained (right) images of duodenum tissue from a *Ctsk-Cre* positive mouse. In the fluorescent image, the nuclei appear as blue with DAPI staining. The cells appear in purple color in the toluidine blue stained image.

Fluorescence White light (toluidine blue)

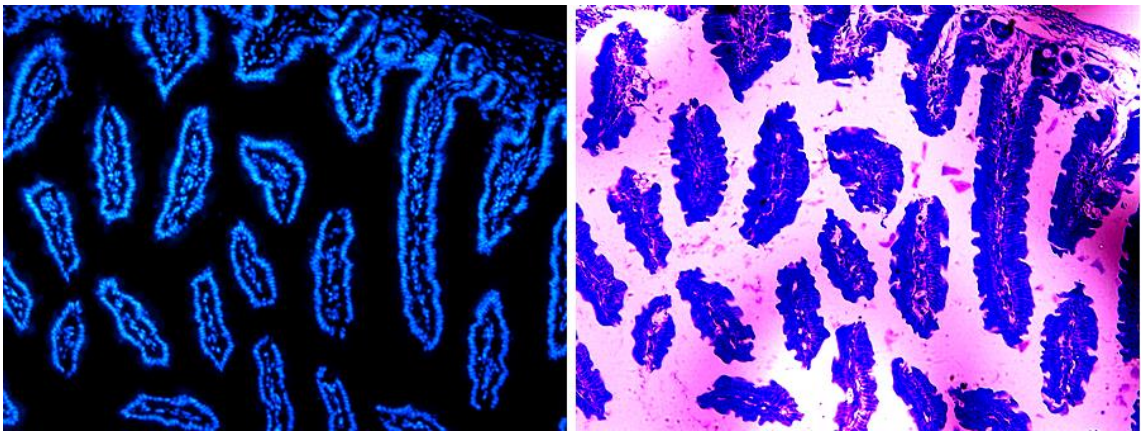

Figure 54: Microscopic images of duodenum tissue from a *Ctsk-Cre* negative mouse. Fluorescent (left) and toluidine blue stained (right) images of duodenum tissue from a *Ctsk-Cre* negative mouse. In the fluorescent image, the nuclei appears as blue with DAPI staining. The cells appear in purple color in the toluidine blue stained image.

Fluorescence White light (toluidine blue)

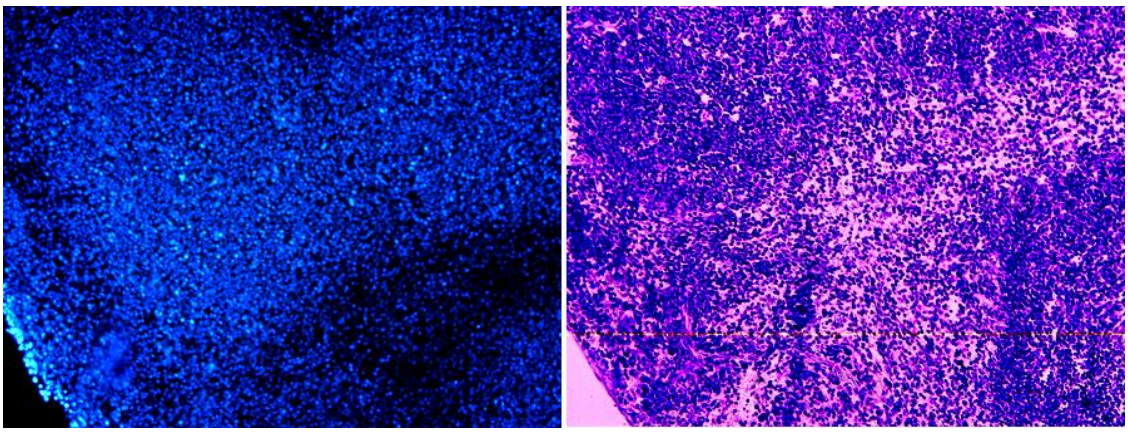

Figure 55: Microscopic images of spleen tissue from a *Ctsk-Cre* positive mouse. Fluorescent (left) and toluidine blue stained (right) images of spleen tissue from a *Ctsk-Cre* positive mouse. In the fluorescent image, the nuclei appear as blue with DAPI staining and a few cells shows red positive. The cells appear in purple color in the toluidine blue stained image.

Fluorescence White light (toluidine blue)

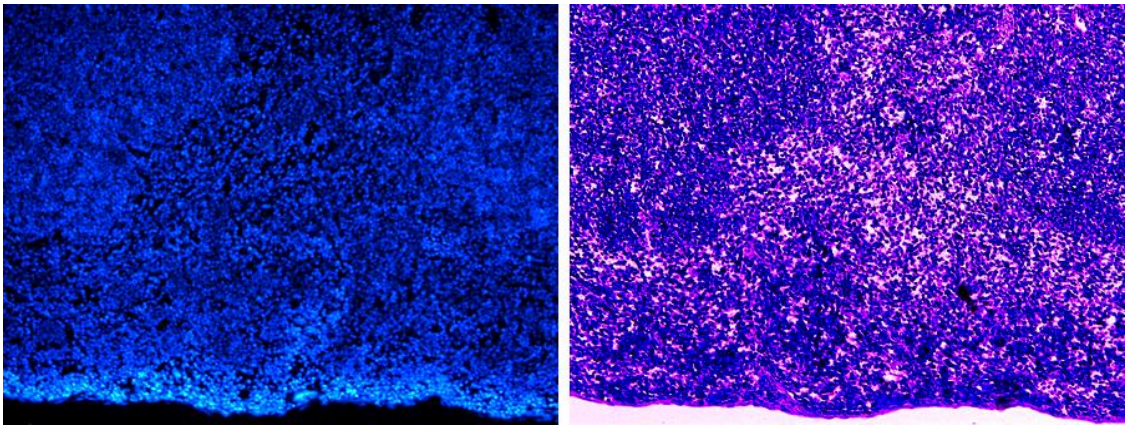

Figure 56: Microscopic images of spleen tissue from a *Ctsk-Cre* negative mouse. Fluorescent (left) and toluidine blue stained (right) images of spleen tissue from a *Ctsk-Cre* negative mouse. In the fluorescent image, nuclei appears as blue with DAPI staining. The cells appear in purple color in the toluidine blue stained image.

3.12. Results of quantitation of positive Cre-expressing cells in the bone and soft tissues of the *Ctsk-Cre* mice by ImageJ cell counting:

To study the effect of Cre-mediated recombination in *Ctsk-Cre* mouse line, fluorescence microscopic analysis of 5um thick sections of the femur bone and soft tissues from the double positive (*Ai9+/Ctsk-Cre+)* mice was performed. The tissue sections were analyzed for positive red color fluorescence which is an indication of Cre recombinase. The total number of cells were counted using ImageJ automated counting tool and the red positive cells in each positive Cre-expressing tissue samples were counted manually. The result of the cell quantitation from positive Cre-expressing tissue are listed in table 4.

The average of percentage of Cre-expression from the studied three *Ctsk-Cre* mice and its standard deviations are listed in table 5.

Figure 57 is Bar chart showing Cre recombinase expression in bone and all tested soft tissues from the three *Ctsk-Cre* mice used in this study.

Ctsk-Cre											
		Bone marrow		**Osteocytes**		**Heart**		**Kidney**		**Liver**	
		Total number of cells	Number of positive cells	Total number of cells	Number of positive cells	Total number of cells	Number of positive cells	Total number of cells	Number of positive cells	Total number of cells	Number of positive cells
Mouse 1	Sample1	4681	7	6	28	958	4	2700	2	1666	3
	Sample2	8503	16	5	30	1655	0	3098	6	1118	0
	Sample3	3526	9	8	33	838	1	2573	4	1325	1
Mouse 2	Sample1	6499	5	2	37	1430	10	3504	6	1509	0
	Sample2	4614	6	6	61	1412	15	3449	3	1633	0
	Sample3	4738	0	5	67	1322	0	3432	1	1628	7
											0
Mouse 3	Sample1	1894	1	8	121	956	0	2981	0	1415	0
	Sample2	4941	4	4	55	1196	0	2652	3	1313	0
	Sample3	4941	3	4	41	951	0	2903	5	1401	0

Table 4: Cell quantitation result from the different tissues of the three *Ctsk-Cre* mice used in this study.

% of Cre exprssion in *Ctsk-Cre* mice tissues[(number of positive cell/Total number of cells) X 100]									
		Bone marrow	**Osteocyte**	**Heart**	**Kidney**	**Liver**	**Brain**	**Duodenum**	**Spleen**
Mouse1	sample								
	1	0.15	21.43	0.42	0.074	0.18	100	0	0
	2	0.19	16.67	0	0.194	0	100	0	0
	3	0.26	24.24	0.12	15.5	0.075	100	0	0
Average		0.2	20.78	0.18	5.256	0.085	100	0	0
Standared deviation		0.055677644	3.8266304	0.21633	8.87177	0.090416	0	0	0
Mouse 2	sample								
	1	0.08	5.41	0.69	0.17	0	100	0	0
	2	0.13	9.84	1.06	0.09	0	100	0	0
	3	0	7.46	0	0.03	0.43	100	0	0
Average		0.07	7.57	0.58333	0.09667	0.143333	100	0	0
Standared deviation		0.065574385	2.2170476	0.53799	0.07024	0.248261	0	0	0
Mouse3	sample								
	1	0.05	6.61	0	0	0	100	0	0
	2	0.081	7.27	0	0.11	0	100	0	0
	3	0.071	9.76	0	0.17	0	100	0	0
Average		0.067333333	7.88	0	0.09333	0	100	0	0
Standared deviation		0.015821926	1.6612345	0	0.08622	0	0	0	0

Table 5: Result of quantitation of positive Cre-expression and its standard deviation from the different tissues of the three *Ctsk-Cre* mice used in this study.

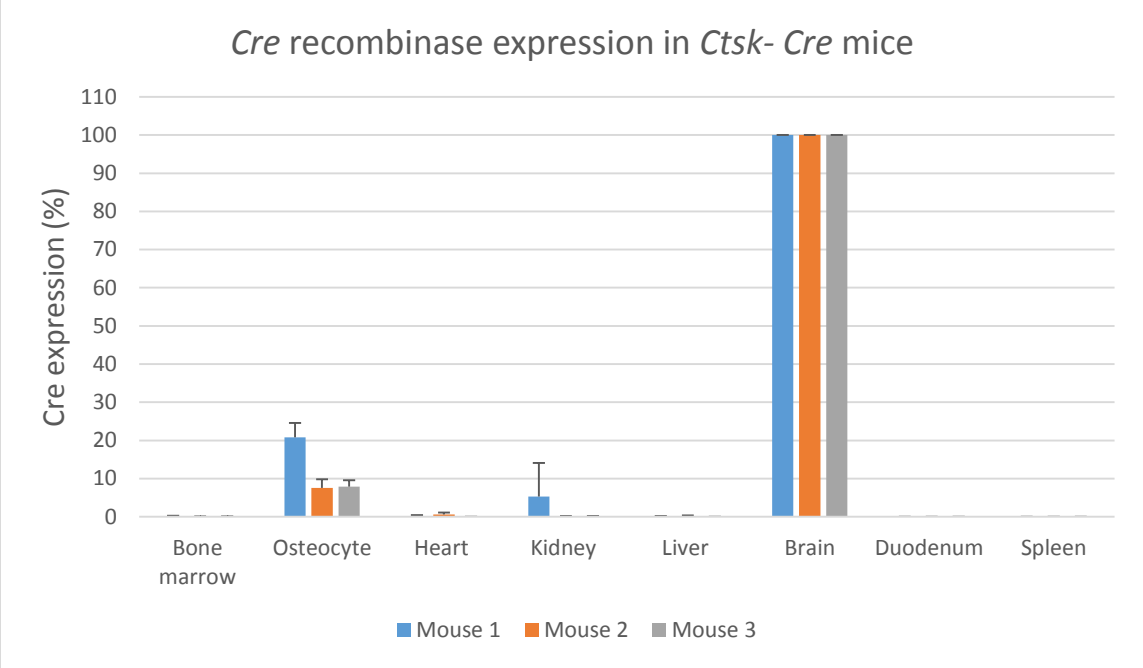

Figure 57: Bar chart showing percentage of Cre recombinase expression from the different tissues of the three *Ctsk-Cre* mice used in this study.

4. Discussion and Conclusion

In this study the tissue specificity and reliability of different bone cell-specific Cre mouse models were tested by crossbreeding them with the *Ai9* Cre reporter mouse line. The bone and soft tissues of the offspring were screened for red fluorescent protein expression, which is the indication for Cre-mediated recombination. Though Cre mouse lines are valuable tools to study site-specific gene recombination in animal models, a literature review indicates that they can be expressed in off target cells [1]. For this reason, Cre mouse lines should be scrutinized for their reliability and selectivity for tissue specific recombination before they are used for actual gene deletion studies. No previous study has been done to determine the reliability and selectivity of bone-cell-specific Cre mouse models. Therefore, our lab was interested to examine them to determine if these Cre mouse models could be used for actual gene deletion experiments in bone tissue. Molecular and histological methods were applied to test the Cre-expression in targeted bone cells and off targeted other soft tissues throughout the body of mouse. To accomplish this goal the *Ai9* reporter was crossed to different bone cell specific Cre mouse lines. In order to test the efficiency of this reporter mouse in bone and soft tissues throughout the mouse body, they were crossed with a global Cre mouse line *E2A* which has a wide range of tissue target including bone and all type of soft tissues. *DMP1-Cre* mouse, where the Cre recombinase is driven by a 14kb fragment of the DMP1 promoter was tested to study its presumed specificity and reliability for late-stage osteoblasts and osteocytes. The tissue sections were examined for red fluorescence in their cells

and the positive cells were quantitated by means of ImageJ software. Likewise, the reliability and selectivity of *Ctsk-Cre* mouse lines were tested for targeted deletion in osteoclasts.

4.1. *Ai9* mouse as Cre reporter line:

In order to test the efficiency and reliability of the *Ai9* allele for studying the effect of Cre-mediated recombination in bone and soft tissues, the reporter mouse was crossbred with the *E2A-Cre* mouse, where E2A is a global promoter that has a wide range of tissue targets and drives the Cre recombinase to all type of cells in the mouse body. The double positive offspring (*Ai9+/E2A+*) were perfused and the bone and soft tissues were analyzed for fluorescence. The fluorescent microscopic analysis of bone tissue showed that osteocytes, osteoclasts and osteoblasts all fluoresced red. But bone marrow was negative in fluorescence which explains that *Ai9* reporter protein is repressed in this compartment. The tested soft tissues such as heart, kidney, liver, spleen, duodenum and brain also showed strong red fluorescence in their cells. These results confirm that the *Ai9* transgene is capable of reporting recombination in all cell types except bone marrow. Thus, if we were to find a lack of fluorescence in our bone-specific Cre screen, we would be able to discount the explanation that the Ai9 was incapable of recombining in those particular cell types. In that sense, the *E2A-Cre* result serves as a positive control.

4.2. Effect of Cre-mediated recombination in the tissues of *DMP1-Cre* mouse line:

DMP1 is a promoter specific for late stage osteoblasts and osteocytes and it drives Cre-expression only to these bone cell types. The *DMP1-Cre* mouse was crossbred with the *Ai9* reporter mouse. The double positive (*Ai9+/DMP1-Cre+)* offspring were perfused and the femur bone and soft tissues such as heart, kidney, liver, brain, duodenum and spleen were analyzed under fluorescence microscopy for red fluorescent protein expression. Three mice samples of 4-6 weeks old were analyzed. Cre-expression in each tissue was quantitated by counting the nuclei of cells of each tissue sample using ImageJ software. The fluorescent microscopic analysis of the bone tissue showed bright red color in the majority of osteocytes (85-88%), and osteoblasts. Marrow showed expression in only 0.5 to 1% of cells. Interestingly, the muscle tissue also showed bright red fluorescence in majority of its cells which cannot be quantitated by counting the total cells (nuclei) since muscle tissue is multi nucleated. There were no red fluorescent cells in the brain and spleen. There were a few positive cells expressing red fluorescence in other soft tissues, heart (0.03-0.7%), kidney (0.24-0.6%), liver (0-0.1%) and duodenum (0.14-5.2%) which is not sufficient to give any phenotypic effect. The results of the study show that *DMP1-Cre* is not a specific model to study gene deletion in osteoblast because of its off targeted expression in muscle tissue.

However, *DMP1-Cre* mouse line is the only available *Cre* model to target osteocytes. To make use of this model for actual gene deletion study in bone tissue, further experiments need to be designed with a mouse that harbors a promoter specific only for muscle tissue (*Muscle-Cre)* so that the deletion can occur only in muscle. If the phenotypic effect of a deletion with *muscle-Cre* gives the same effect with that of *Dmp1-Cre,* it might indicates that the gene of interest has functional significance in muscle rather than bone. On the other hand, the red fluorescence in the muscle tissue does not necessarily indicate that there is *DMP1-Cre* expression in the muscle at the time of sacrifice. Certain genes are temporarily expressed and then diminish during the embryonic stage. There is a possibility that *DMP1* gene is transiently expressed in the muscle during embryonic development, which would have lasting effects on all daughter cells. The cells remain red because the recombination of the mTomato allele is irreversible even after *DMP1* expression is turned off. To investigate on this, we can make use of a next generation of Cre model in which the timing of Cre activity in nucleus can be controlled. This is accomplished by fusing the Cre protein with an estrogen receptor mutant protein. The estrogen receptor portion of the fusion protein sequesters the protein in the cytosol, away from the nucleus. Consequently, no Cre-DNA activity occurs. However, when the cell is exposed to the estrogen analog tamoxifen, the fusion protein is stimulated to translocate to the nucleus, where it can exert its recombination activity [2, 11]. Our lab is interested to conduct a future study with these mice that harbor this Cre-estrogen mutant protein—called CreERt2—driven by the Dmp1 promoter (osteocyte

selective) in conjunction with the Ai9 reporter, to assess whether the expression in muscle cell is limited to embryonic stage of *DMP1-Cre* mouse.

4.3. Effect of Cre-mediated recombination in the tissues of *Ctsk-Cre* mouse line:

Ctsk is a promoter specific for osteoclasts and it presumably drives Cre-expression only tin osteoclasts. The *Ctsk-Cre* mouse was cross bred with the *Ai9* reporter mouse. The double positive (*Ai9+/Ctsk-Cre+)* offspring were perfused and the femur bone and soft tissues such as heart, kidney, liver, brain, duodenum and spleen were analyzed under fluorescent microscope for red fluorescent expression. Three mice samples of 4-6 weeks old were analyzed. Cre-expression in each tissue was quantitated by counting the nuclei of cells of each tissue sample using ImageJ software. The fluorescent microscopic analysis of the bone tissue showed bright red color on cells on the bone surface where osteoclasts are located. However it is not possible to quantitate total number of osteoclasts present in each sample since they are multinucleated and it is difficult to identify them. A surprising number of osteocytes expressed the fluorescent protein (7-20.1%). Marrow showed expression in only 0.07- to 0.2% of its cells. There were no red fluorescent cells in duodenum and spleen. There were very few number of cells expressed in other soft tissues, heart (0 – 0.5%), kidney (0.09 – 5.3%), liver (0 – 0.1%), which is not sufficient to give any phenotypic effect. However, this study has revealed that *Ctsk-Cre* is expressed in brain since100% of the brain cells were turned to bright red color. The results of is

study shows that *Ctsk-Cre* is not a specific model to study gene deletion in osteoclasts because of its nonspecific expression in brain tissue.

Trap-Cre is another mouse model available to target gene deletion in osteoclasts which needs to be tested in similar way. To make use of *Ctsk-Cre* for actual gene deletion study in bone tissue, further experiments need to be designed with a mouse that harbor a promoter specific only for brain tissue (*brain-Cre)* so that the deletion occurs only in brain. If the phenotypic effect of a deletion with '*brain-Cre'* gives the same effect with that of *'bone-Cre',* it implies that the gene of interest has functional significance in brain.

As previously explained, the red fluorescence in the brain tissue does not necessarily indicate that there is *Ctsk-Cre* expression in the brain at the time of sacrifice. It could be the transient expression of *Ctsk* gene in brain during embryonic development, which would have lasting effects on all daughter cells. However, the cells remain red because the recombination of the mTomato allele is irreversible even after *Ctsk* expression is turned off. To investigate this, a next generation of Cre model *Ctsk-Cre-ERt2* has to be constructed since this mouse model has not been constructed the moment.

This study has revealed that *DMP1* gene is expressed in muscle tissue and *Ctsk* gene is expressed in brain tissue of the respective Cre mouse lines though it is not certain whether the expression is limited to the embryonic developmental

stage. It has opened vast areas for further research such as whether these genes are expressed in postnatal life, if so, what are the functional roles of these genes in those expressed soft tissues. If these questions are answered, these bone cell specific Cre mouse models can still be utilized to delete and study a gene of interest in bone cells.

5. References

[1] Abremski K, Hoess R, Bacteriophage P1 site-specific recombination. Purification and properties of the Cre recombinase protein, 10; 259(3):1509-14, 1984 February.

[2] Hoess RH, Abremski K, Mechanism of strand cleavage and exchange in the Cre-lox site-specific recombination system, Journal of Molecular biology 5; 181(3):351-62, 1985 February.

[3] Anton M, Graham FL, Site-specific recombination mediated by an adenovirus vector expressing the Cre recombinase protein: a molecular switch for control of gene expression. J Virol, 1995 August, 69(8):4600-4606.

[4] Sauer B, Identification of cryptic lox sites in the yeast genome by selection for Cre- mediated chromosome translocations that confer multiple drug resistance, Journal of Molecular Biology, 223(4): 911-928, 1992.

[5] Nagy A, Cre Recombinase: The Universal Reagent for Genome Tailoring, Genesis 26:99–109, 2000.

[6] Abremski K, Hoess R, and Stemberg N, Studies on the properties of P1 site - specific recombination: Evidence for topologically unlinked products following recombination, Cell, 32(4): 1301-11, 1983.

[7] Furth, A Priscilla, Conditional Control of Gene Expression in the Mammary Gland, Journal of mammary gland biology and neoplasia, 2 (4): 363-83,1997.

[8] Lee S, Good planning and serendipity: exploiting the Cre/Lox system in the testis, Reproduction the journal of the society for reproduction and fertility, Reproduction, 141 (2): 151-161, 2010.

[9] Bilezikian J, Raisz L, John Martin T, Principles of Bone Biology (3rd edition), 1:20-25, 2008©.

[10] Burr B. David, Allen T Matthew, Basic and applied bone biology, Elsevier Inc., 1:34-41, 2014©.

[11] Neve A, Corrado A, Cantatore F, Osteocytes: central conductors of bone biology in normal and pathological conditions, Acta Physiologica, 204:317-330, 2012.

[12] Kalajzic I, Braut A, Guo D, Jiang X, Kronenberg MS, Mina M, Harris MA, Harris SE, Rowe DW, Dentin matrix protein 1 expression during osteoblastic differentiation, generation of an osteocyte GFP-transgene, Bone 35(1):74- 82, 2004.

[13] Fen JQ, Zhang J, Dallas SL, Lu Y, Chen S, Tan X, Owen M, Harris SE, MacDougall M, Dentin matrix protein 1, a target molecule for Cbfa1 in bone, is a unique bone marker gene, Bone, 35(1):74-82, 2004.

[14] Turan S, Aydin C, Bereket A, Akcay T, Güran T, Yaralioglu BA, Bastepe M, Jüppner H, Identification of a Novel Dentin Matrix Protein-1 (DMP-1) Mutation and Dental Anomalies in a Kindred with Autosomal Recessive Hypophosphatemia, Bone, 46(2): 402-409, 2012.

[15] Madisen L, Zwingman TA, Sunkin SM, Oh SW, Zariwala HA, Gu H, Ng LL, Palmiter RD, Hawrylycz MJ, Jones AR, Lein ES, Zeng H, A robust and high- throughput Cre reporting and characterization system for the whole mouse brain, Nature neuroscience, 13:133-140, 2010.

[16] Sanchez-Fernandez MA, Sbacchi S, Correa-Tapia M, Naumann R, Klemm J, Chambon P, Al-Robaiy S, Blessing M, Hoflack B., Transgenic Mice for a Tamoxifen-Induced, Conditional Expression of the Cre Recombinase in Osteoclasts, plos one, 7(5): e37592, 2012.

[17] Guo C, Yang W, Lobe C, A Cre Recombinase Transgene with Mosaic, Widespread Tamoxifen-Inducible Action, Genesis 32:8–18, 2002.

[18] Kawamoto T, Use of anew adhesive film for the preparation of multi-purpose fresh-frozen sections from hard tissues, whole animals, insects and plants. Archives of Histology and Cytology, 66(2):123-143, 2003.

[19] Datta HK, Ng WF, Walker JA, Tuck SP, Varanasi SS, The cell biology of bone metabolism, J of Clinical Pathology, 61(5):577-87, 2008.

[20] Lu Y, Xie Y, Zhang S, Dusevich V, Bonewald LF, Feng JQ, DMP1-targeted Cre expression in odontoblasts and osteocytes, Journal of Dental Research, 86(4):320-5, 2007.

[21] Chiu WS, McManus JF, Notini AJ, Cassady AI, Zajac JD, Davey RA, Transgenic Mice That Express Cre Recombinase in Osteoclast, genesis 39:178–185, 2004.

[22] Powell WF Jr, Barry KJ, Tulum I, Kobayashi T, Harris SE, Bringhurst FR, Pajevic PD, Targeted ablation of the PTH/PTHrP receptor in osteocytes impairs bone structure and homeostatic calcemic responses, J Endocrinology, 209(1):21-32, 2011.

[23] Lazorchak AS, Wojciechowski J, Dai M, Zhuang Y, E2A Promotes the Survival of Precursor and Mature B Lymphocytes, J Immunol. 2006 Aug 15; 177(4):2495-504.

[24] Zhao J, Nassar MA, Gavazzi I, Wood JN, Tamoxifen-inducible NaV1.8-CreERT2 recombinase activity in nociceptive neurons of dorsal root ganglia, Genesis. 2006 Aug; 44(8):364-71.

[25] Lakso M, Pichel JG, Gorman JR, Sauer B et al, Efficient in vivo manipulation of mouse genomic sequences at the zygote stage, Proc Natl Acad Sci U S A,93(12):5860-5, 1996 Jun 11.

[26] Hayashi S, McMahon AP. Efficient recombination in diverse tissues by a tamoxifen-inducible form of Cre: a tool for temporally regulated gene activation/inactivation in the mouse, 244(2)305-18, 2002 Apr 15.

[27] R H Hoess, A Wierzbicki, K Abremski, The role of the loxP spacer region in P1 site-specific recombination,.Nucleic Acids Res, 14(5): 2287–2300, 1986 March 11.

[28] Kondo N, Ogose A, Tokunaga K et al., Osteoinduction with highly purified beta-tricalcium phosphate in dog dorsal muscles and the proliferation of osteoclasts before heterotopic bone formation. Biomaterials. 27(25):4419-27, 2006 September.

[29] Rossant Janet, McMahon Andrew, Cre-ating mouse mutants—a meeting review on conditional mouse genetics, Genes& Development, 13:142-145, 1999.

[30] Shimshek, D.R., Kim, J., Hübner, M.R., Spergel, D.J., Buchholz, F., Casanova, E., Stewart, A.F., Seeburg, P.H. and Sprengel, R, Codon-improved Cre recombinase (iCre) expression in the mouse. Genesis, 32: 19–26. doi: 10.1002/gene.10023, 2000.

[31] Moses, K. A., DeMayo, F., Braun R. M., Reecy, J. L. and Schwartz, R. J, Embryonic expression of an Nkx2-5/Cre gene using ROSA26 reporter mice. Genesis, 31: 176–180. doi: 10.1002/gene.10022, 2001.

[32] Kos, C. H, Methods in Nutrition Science: Cre/loxP System for Generating Tissue-specific Knockout Mouse Models. Nutrition Reviews, 62: 243–246, 2004.

[33] Truett G.E, Heeger P, Mynat R.L, Truett A. A,Walker J.A, Warman M.L, Preparation of PCR-quality mouse genomic DNA with hot sodium hydroxide and tris (HotSHOT), Biotechniques, 29:52-54(July 2000)

[34] Ferreira Tiago, Rasband Wayne, ImageJ User's guide, 1.46r:1-4, October 2012.

[35] Labno Christine, 'Basic Intensity Quantification with ImageJ', University of Chicago, http://www.digital.bsd.uchicago.edu, on and after 2014.

[36] Automatic nuclei counting plugin for ImageJ', center for Bio-Image Informatics, http://www.bioimage.ucsb.edu/automatic-nuclei-counter-plug-in-for-imagej, on and after 2014.

[37] Jensen C Ellen, ‘Quantitative Analysis of Histological Staining and Fluorescence using ImageJ’, The Anatomical record 296:379-381, 2013.

[38] Jones ME1, Kondo M, Zhuang Y, A tamoxifen inducible knock-in allele for investigation of E2A function, BMC Developmental Biology 9:51, 2009.

6. Curriculum Vitae

Anuradha Valiya Kambrath

Education

MS in Biochemistry and Molecular Biology, Indiana University, 2015. Thesis: Testing the reliability and selectivity of different bone-cell- specific Cre-expressing mouse models for studying bone cell metabolism.

Graduate Certification in Biotechnology Training Program, Indiana University, 2010, involves laboratory based courses in Molecular biology, Cell Biology and Biotechnology.

Master of Science in Applied Microbiology, Madras University, India, 2001. Thesis: Ocular surface infections-a microbiological study.

Bachelor of Science in Zoology with Botany and Chemistry as subsidiaries Kannur University, India, 1999.

Experiences

Indiana University, Indianapolis (Aug 2012- October 2014):
Worked as a student trainee, and pursued Master's thesis project in the Department of Biochemistry, Indiana University, Indianapolis, where I have been involved in experiments including Molecular Biology and immune-histochemical techniques. I have also involved in laboratory animal works such as ear notching of mice for tagging, injection, perfusion and organ collection. I am experienced in molecular biology techniques such as DNA extraction, PCR, genotyping. I have been receiving great deal of experience in Cryosectioning, staining, histochemical analysis and fluorescent microscopy analysis of bone and other tissues from mice.

Indiana University, Indianapolis (Aug 2010- November 2010):
Worked as a volunteer technician in Indiana Center for Vascular Biology and Medicine, IU School of Medicine, Indianapolis, where I have performed molecular biology techniques such as DNA extraction from mouse tail snips, PCR with genotype specific primers, Immuno-histochemical analysis by fluorescent and calorimetric microscopy analysis of lung and eye samples and in vitro cell culture experiments.

Medwin Hospital, Hyderabad, India (April 2005 to October 2005):
Worked as a Research Associate in the Department of Biochemistry, where I was Involved in protein sequence analysis and drug designing. I have been involved in the project work entitled 'Target identification of ACE gene- An *Insilco* approach' where we applied Bioinformatics tools and database to find out the potential ligand binding site for ACE gene followed by drug designing.

Doctor’s Laboratory, Payyanur, India (September 2001 to August 2002): Worked as a technician where I was involved in routine Microbiology laboratory techniques such as, aseptic techniques, media preparation, and culturing and antibiotic sensitivity tests.

Pariyaram Medical College, Kannur, India (May 2000 to August 2000): Worked as an intern in the Department of Microbiology, Pariyaram Medical College, India, where I have performed microbiology techniques such as preparation of bacterial and fungal media, culturing, colony isolation and identification and antibiotic sensitivity tests.